© 2015 IJSRSET | Volume 1 | Issue 3 | Print ISSN: 2395-1990 | Online ISSN: 2394-4099
Themed Section: Engineering and Technology

Advances in fracture and numerical analysis of piezoelectric materials

Yi Xiao

Research School of Engineering, Australian National University, Acton, ACT 2601, Australia

ABSTRACT

This paper presents an overview of crack problems and numerical analysis of piezoelectric materials. Developments in Green's function, Crack problem, finite element, and boundary element formulation of piezoelectric materials are described. Finally, a brief summary of the approaches discussed is provided and future trends in this field are identified.

Keywords: Piezoelectric materials, Green's function, Fracture mechanics

I. INTRODUCTION

Piezoelectric material is such that when it is subjected to a mechanical load, it generates an electric charge. This effect is usually called the "piezoelectric effect". Conversely, when piezoelectric material is stressed electrically by a voltage, its dimensions change. This phenomenon is known as the "inverse piezoelectric effect". The study of piezoelectricity was initiated by J. and P. Curie in 1880 [1]. They found that certain crystalline materials generate an electric charge proportional to a mechanical stress. Since then new theories and applications of the field have been constantly advanced [2-10]. Voigt [2] developed the first complete and rigorous formulation of piezoelectricity in 1890. Since then several books on the phenomenon and theory of piezoelectricity have been written. Among them are the references by Cady [3], Tiersten [4], Parton and Kudryavtsev [5], Ikeda [6], Rogacheva [7], Qin [8-11], and Qin and Yang [12]. The first of these [2] treated the physical properties of piezoelectric crystals as well as their practical applications, the second [3] dealt with the linear equations of vibrations in piezoelectric materials, and the third and fourth [4, 5] gave a more detailed description of the physical properties of piezoelectricity. Rogacheva [7] presented general theories of piezoelectric shells. Qin [8-11] discussed Green's functions, advanced theory, and fracture mechanics of piezoelectric materials as well as applications to bone remodelling. Micromechanics of the piezoelectricity were discussed in [12]. These advances have resulted in a great number of publications including journal and conference papers. These include but not limit to applications to Branched crack problems[13-15], experimental investigation of bone materials [16-21], multi-field problems of bone remodelling [22-29], decay analysis of dissimilar laminates [30], moving crack problems [31], anti-plane crack problems [32, 33], fibre-pull out [34], fibre-push out [35-37], problems of frog Sartorius muscles [38], effective property evaluation [39-42], Green's function analysis [43-50], derivation of general solutions [51-54], boundary element analysis [55-62], micro-macro crack interaction problems [63], Trefftz finite element analysis [64-69], crack-inclusion problems [70, 71], crack growth problem [72, 73], multi-crack problems [74], crack-interface problems [75-77], closed crack-tip analysis [78], crack-path selection [79], penny-shaped crack analysis [80, 81], logarithmic singularity analysis [82], multi-layer piezoelectric actuator [83, 84], Symplectic mechanics analysis [85], interlayer stress analysis [86], coupled thermo-electro-chemo-mechanical analysis [87], and damage analysis [88, 89].

Based on the analysis above, the present review consists of six sections. Green's functions are described

in Section 2. Section 3 focuses on crack problems of piezoelectric materials. The application of finite elements and boundary elements to piezoelectric materials are discussed in Sections 4-5. Finally, a brief summary on these sections is provided and areas that need further research are identified.

II. Green's function of half-plane and biomaterial problems

This section is concerned with the application of the derivation of Green's function for a half-plane or bimaterial problem of a magnetoelectroelastic solid.

II.1 Basic formulations

The governing equations and general solutions of 2D magnetoelectroelastic solids where all fields are functions of x_1 and x_2 only are here summarized briefly. Throughout this paper the shorthand[8, 47] and the fixed Cartesian coordinate system (x_1, x_2, x_3) are adopted. Lower-case Latin subscripts always range from 1 to 3, upper-case Latin subscripts range from 1 to 5, and the summation convention is used for repeating subscripts unless otherwise indicated. In the stationary case when no free electric charge, electric current, and body force are assumed to exist, the complete set of governing equations for uncoupled electromagnetoelastic problems is [10]:

$$\Sigma_{iJ,i} = 0 \tag{1}$$

together with

$$\Sigma_{iJ} = E_{iJMn} U_{M,n} \tag{2}$$

in which

$$\Sigma_{iJ} = \begin{cases} \sigma_{ij}, & J \le 3, \\ D_i, & J = 4, \\ B_i, & J = 5, \end{cases} \qquad U_M = \begin{cases} u_m, & M \le 3, \\ \phi, & M = 4, \\ \varpi, & M = 5, \end{cases} \tag{3}$$

$$E_{iJMn} = \begin{cases} C_{ijmn}, & J, M \le 3, \\ e_{nij}, & J \le 3, M = 4, \\ q_{nij}, & J \le 3, M = 5, \\ e_{imn}, & J = 4, M \le 3, \\ -\kappa_{in}, & J = 4, M = 4, \\ -a_{in}, & J = 4, M = 5, \\ q_{imn}, & J = 5, M \le 3, \\ -a_{in}, & J = 5, M = 4, \\ -\mu_{in} & J = 5, M = 5, \end{cases} \tag{4}$$

where σ_{ij}, D_i, and B_i are elastic stress tensors, electric displacement vectors, and magnetic induction vectors respectively; u_m, ϕ, and ϖ denote elastic displacement vector, electric potential, and magnetic potential; C_{ijmn} are elastic moduli, e_{nij} are piezoelectric coefficients, q_{nij} are piezomagnetic coefficients, a_{in} are magnetoelectric coefficients, κ_{in} are dielectric constants, and μ_{in} are magnetic permeability. A general solution to eqn (1) can be expressed as [90]:

$$\mathbf{U} = 2\,\mathrm{Re}[\mathbf{A}\mathbf{f}(\mathbf{z})\mathbf{q}] \tag{5}$$

with

$$\mathbf{A} = [\mathbf{A}_1\ \mathbf{A}_2\ \mathbf{A}_3\ \mathbf{A}_4\ \mathbf{A}_5]$$
$$\mathbf{f}(\mathbf{z}) = \langle f(z_\alpha) \rangle = \mathrm{diag}[f(z_1)\ f(z_2)\ f(z_3)\ f(z_4)\ f(z_5)]$$
$$\mathbf{q} = \{q_1\ q_2\ q_3\ q_4\ q_5\}^T$$
$$z_i = x_1 + p_i x_2$$

in which "Re" stands for the real part of the complex number, the prime (′) denotes differentiation with respect to the argument, **q** denotes unknown constants to be found by boundary conditions, **f** is an arbitrary function to be determined, and p_i and **A** are constants determined by

$$[\mathbf{Q} + (\mathbf{R} + \mathbf{R}^T) p_i + \mathbf{T} p_i^2]\mathbf{A}_i = 0 \tag{6}$$

in which the superscript "*T*" denotes the transpose, and **Q**, **R** and **T** are 5×5 matrices defined by

$$(\mathbf{Q})_{IK} = E_{1IK1},\ (\mathbf{R})_{IK} = E_{1IK2},\ (\mathbf{T})_{IK} = E_{2IK2}. \tag{7}$$

The stress-electric displacement-magnetic induction (SEDMI), **Σ**, obtained from Eq. (2) can be written as

$$\mathbf{\Sigma}_{1J} = -\boldsymbol{\varphi}_{J,2},\quad \mathbf{\Sigma}_{2J} = \boldsymbol{\varphi}_{J,1} \tag{8}$$

where **φ** is the SEDMI function given as

$$\boldsymbol{\varphi} = 2\,\mathrm{Re}[\mathbf{B}\mathbf{f}(\mathbf{z})\mathbf{q}] \tag{9}$$

with

$$\mathbf{B} = \mathbf{R}^T\mathbf{A} + \mathbf{T}\mathbf{A}\mathbf{P} = -(\mathbf{Q}\mathbf{A} + \mathbf{R}\mathbf{A}\mathbf{P})\mathbf{P}^{-1}$$
$$\mathbf{P} = \langle p_\alpha \rangle = \mathrm{diag}[p_1\ p_2\ p_3\ p_4\ p_5]. \tag{10}$$

II.2 Green's function for half-plane and bimaterial problems

The half-plane or bimaterial interface considered in this section is different from those reported in the literature [50, 91, 92]. The half-plane boundary (or bimaterial) is in the vertical ($x_1 = 0$ on the boundary in our analysis) rather than the horizontal direction (see Fig. 1). It is obvious that $z_k = x_1 + p_k x_2$ becomes a real number on the horizontal boundary $x_2 = 0$. However, z_k is, in general, neither a real number nor a pure imaginary number on the vertical boundary $x_1 = 0$, which complicates the related mathematical derivation. To

bypass this problem, a new coordinate variable is introduced:

$$z_k^* = z_k / p_k . \tag{11}$$

In this case z_k^* is a real number on the vertical boundary $x_1 = 0$. This coordinate transformation is used for both the half-plane and bimaterial problem below.

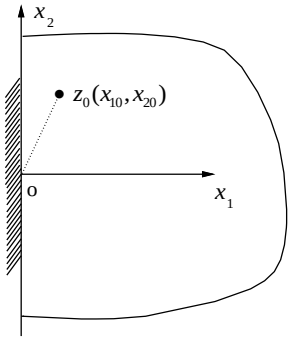

Fig. 1 Magnetoelectroelastic half-plane

II.2.1 Green's function for full space

For an infinite magnetoelectroelastic solid subjected to a line force $\mathbf{q}_0$ and a line dislocation **b** both located at $z_0(x_{10}, x_{20})$ (see Fig. 1), the solution in the form of Eq. (5) and (9) is [55]:

$$\mathbf{U} = \frac{1}{\pi}\mathrm{Im}[\mathbf{A}\langle \ln(z_\alpha^* - z_{\alpha 0}^*)\rangle \mathbf{q}],$$
$$\boldsymbol{\varphi} = \frac{1}{\pi}\mathrm{Im}[\mathbf{B}\langle \ln(z_\alpha^* - z_{\alpha 0}^*)\rangle \mathbf{q}] \tag{12}$$

where **q** is a complex vector to be determined. Since $\ln(z_\alpha^* - z_{\alpha 0}^*)$ is a multi-valued function we introduce a cut along the line defined by $x_2 = x_{20}$ and $x_1 \le x_{10}$. Using the polar coordinate system (r, θ) with its origin at $z_0(x_{10}, x_{20})$ and with $\theta = 0$ being parallel to the x_1-axis, the solution (12) applies to

$$-\pi < \theta < \pi, \qquad r > 0. \tag{13}$$

Therefore

$$\ln(z_\alpha^* - z_{\alpha 0}^*) = \ln r \pm i\pi, \text{ at } \theta = \pm\pi \text{ for } \alpha = 1\text{-}5. \tag{14}$$

Owing to this relation, Eq. (12) must satisfy the conditions

$$\mathbf{U}(\pi) - \mathbf{U}(-\pi) = \mathbf{b}, \quad \boldsymbol{\varphi}(\pi) - \boldsymbol{\varphi}(-\pi) = \mathbf{q}_0 \tag{15}$$

which lead to

$$2\,\mathrm{Re}(\mathbf{Aq}) = \mathbf{b}, \qquad 2\,\mathrm{Re}(\mathbf{Bq}) = \mathbf{q}_0 . \tag{16}$$

This can be written as

$$\begin{bmatrix} \mathbf{A} & \overline{\mathbf{A}} \\ \mathbf{B} & \overline{\mathbf{B}} \end{bmatrix} \begin{Bmatrix} \mathbf{q} \\ \overline{\mathbf{q}} \end{Bmatrix} = \begin{Bmatrix} \mathbf{b} \\ \mathbf{q}_0 \end{Bmatrix}. \tag{17}$$

It follows from the relation

$$\begin{bmatrix} \mathbf{B}^T & \mathbf{A}^T \\ \overline{\mathbf{B}}^T & \overline{\mathbf{A}}^T \end{bmatrix} \begin{bmatrix} \mathbf{A} & \overline{\mathbf{A}} \\ \mathbf{B} & \overline{\mathbf{B}} \end{bmatrix} = \begin{bmatrix} \mathbf{I} & 0 \\ 0 & \mathbf{I} \end{bmatrix} \tag{18}$$

that

$$\begin{Bmatrix} \mathbf{q} \\ \overline{\mathbf{q}} \end{Bmatrix} = \begin{bmatrix} \mathbf{B}^T & \mathbf{A}^T \\ \overline{\mathbf{B}}^T & \overline{\mathbf{A}}^T \end{bmatrix} \begin{Bmatrix} \mathbf{b} \\ \mathbf{q}_0 \end{Bmatrix}. \tag{19}$$

Hence

$$\mathbf{q} = \mathbf{A}^T \mathbf{q}_0 + \mathbf{B}^T \mathbf{b}. \tag{20}$$

II.2.2 Green's function for half-space

Let the material occupy the region $x_1 > 0$, and a line force-charge $\mathbf{q}_0$ and a line dislocation **b** apply at $z_0(x_{10}, x_{20})$. To satisfy the boundary conditions on the infinite straight boundary of the half-plane (see Fig. 1), the solution should be modified as follows

$$\mathbf{U} = \frac{1}{\pi}\mathrm{Im}\{\mathbf{A}\langle \ln(z_\alpha^* - z_{\alpha 0}^*)\rangle \mathbf{q}\} + \sum_{\beta=1}^{5}\frac{1}{\pi}\mathrm{Im}\{\mathbf{A}\langle \ln(z_{\alpha 0}^* - \bar{z}_{\beta 0}^*)\rangle \mathbf{q}_\beta\}, \tag{21}$$

$$\boldsymbol{\varphi} = \frac{1}{\pi}\mathrm{Im}\{\mathbf{B}\langle \ln(z_\alpha^* - z_{\alpha 0}^*)\rangle \mathbf{q}\} + \sum_{\beta=1}^{5}\frac{1}{\pi}\mathrm{Im}\{\mathbf{B}\langle \ln(z_{\alpha 0}^* - \bar{z}_{\beta 0}^*)\rangle \mathbf{q}_\beta\} \tag{22}$$

where **q** is given in Eq. (20) and $\mathbf{q}_\beta$ are unknown constants to be determined.

Consider first the case in which the surface $x_1 = 0$ is traction-free, so that [8]

$$\boldsymbol{\varphi} = 0 \qquad \text{at } x_2 = 0. \tag{23}$$

Substituting Eq. (22) into Eq. (23) yields

$$\boldsymbol{\varphi} = \frac{1}{\pi}\mathrm{Im}\{\mathbf{B}\langle \ln(x_2 - z_{\alpha 0}^*)\rangle \mathbf{q}\} + \sum_{\beta=1}^{5}\frac{1}{\pi}\mathrm{Im}\{\mathbf{B}\langle \ln(x_2 - \bar{z}_{\beta 0}^*)\rangle \mathbf{q}_\beta\} = 0 \tag{24}$$

Noting that $\mathrm{Im}(f) = -\mathrm{Im}(\bar{f})$, we have

$$\mathrm{Im}\{\mathbf{B}\langle \ln(x_2 - z_{\alpha 0}^*)\rangle \mathbf{q}\} = -\mathrm{Im}\{\overline{\mathbf{B}}\langle \ln(x_2 - \bar{z}_{\alpha 0}^*)\rangle \overline{\mathbf{q}}\}, \tag{25}$$

and

$$\langle \ln(x_2 - z_{\alpha 0}^*)\rangle = \sum_{\beta=1}^{5} \ln(x_2 - z_{\beta 0}^*)\mathbf{I}_\beta , \tag{26}$$

where

$$\mathbf{I}_\beta = \langle \delta_{\beta\alpha} \rangle = \mathrm{diag}[\delta_{\beta 1}, \delta_{\beta 2}, \delta_{\beta 3}, \delta_{\beta 4}, \delta_{\beta 5}]. \tag{27}$$

Eq. (24) now yields

$$\mathbf{q}_\beta = \mathbf{B}^{-1}\overline{\mathbf{B}}\mathbf{I}_\beta \overline{\mathbf{q}} = \mathbf{B}^{-1}\overline{\mathbf{B}}\mathbf{I}_\beta (\overline{\mathbf{A}}^T \mathbf{q}_0 + \overline{\mathbf{B}}^T \mathbf{b}). \tag{28}$$

If the boundary $x_1 = 0$ is a rigid surface, then

$$\mathbf{U} = 0, \qquad \text{at } x_2 = 0. \tag{29}$$

The same procedure shows that the solution is given by Eqs. (21) and (22) with

$$\mathbf{q}_\beta = \mathbf{A}^{-1}\overline{\mathbf{A}}\mathbf{I}_\beta(\overline{\mathbf{A}}^T\mathbf{q}_0 + \overline{\mathbf{B}}^T\mathbf{b}). \quad (30)$$

Therefore the final version of the Green's function can be written in terms of z_k as

$$\mathbf{U} = \frac{1}{\pi}\mathrm{Im}\{\mathbf{A}\langle \ln(z_\alpha - z_{\alpha 0})/p_\alpha\rangle\mathbf{q}\} + \sum_{\beta=1}^{5}\frac{1}{\pi}\mathrm{Im}\{\mathbf{A}\langle \ln(z_\alpha/p_\alpha - \bar{z}_{\beta 0}/\bar{p}_\beta)\rangle\mathbf{q}_\beta\} \quad (31)$$

$$\boldsymbol{\varphi} = \frac{1}{\pi}\mathrm{Im}\{\mathbf{B}\langle \ln(z_\alpha - z_{\alpha 0})/p_\alpha\rangle\mathbf{q}\} + \sum_{\beta=1}^{5}\frac{1}{\pi}\mathrm{Im}\{\mathbf{B}\langle \ln(z_\alpha/p_\alpha - \bar{z}_{\beta 0}/\bar{p}_\beta)\rangle\mathbf{q}_\beta\}. \quad (32)$$

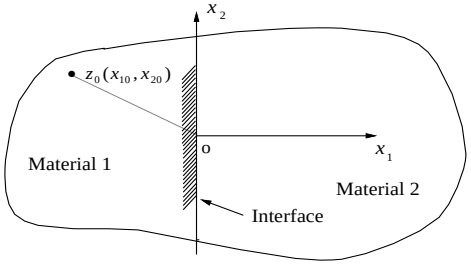

Fig. 2 Magnetoelectroelastic bimaterial plate

II.2.3 Green's function for a bimaterial problem

We now consider a bimaterial solid whose interface is on x_2-axis($x_1 = 0$). It is assumed that the left half-plane ($x_1 < 0$) is occupied by material 1, and the right half-plane ($x_1 > 0$) by material 2 (Fig. 2). They are rigidly bonded together so that

$$\mathbf{U}^{(1)} = \mathbf{U}^{(2)}, \quad \boldsymbol{\varphi}^{(1)} = \boldsymbol{\varphi}^{(2)}, \text{ at } x_1 = 0 \quad (33)$$

where the superscripts (1) and (2) label the quantities relating to materials 1 and 2 respectively. The equality of traction continuity comes from the relations $\mathbf{t} = \partial\boldsymbol{\varphi}/\partial s$. When points along the interface are considered, integration of $\mathbf{t}^{(1)} = \mathbf{t}^{(2)}$ provides Eq. $(33)_2$ since the integration constants corresponding to rigid motion can be neglected.

For a magnetoelectroelastic bimaterial plate subjected to a line force-charge $\mathbf{q}_0$ and a line dislocation $\mathbf{b}$ both located in the left half-plane at $z_0(x_{10}, x_{20})$ (Fig. 2), the solution may be assumed, in a similar treatment to that in the half-plane problem, in the form

$$\mathbf{U}^{(1)} = \frac{1}{\pi}\mathrm{Im}\{\mathbf{A}^{(1)}\langle \ln(z_\alpha^{*(1)} - z_{\alpha 0}^{*(1)})\rangle\mathbf{q}\} + \sum_{\beta=1}^{5}\frac{1}{\pi}\mathrm{Im}\{\mathbf{A}^{(1)}\langle \ln(z_\alpha^{*(1)} - \bar{z}_{\beta 0}^{*(1)})\rangle\mathbf{q}_\beta^{(1)}\}, \quad (34)$$

$$\boldsymbol{\varphi} = \frac{1}{\pi}\mathrm{Im}\{\mathbf{B}\langle \ln(z_\alpha - z_{\alpha 0})/p_\alpha\rangle\mathbf{q}\} + \sum_{\beta=1}^{5}\frac{1}{\pi}\mathrm{Im}\{\mathbf{B}\langle \ln(z_\alpha/p_\alpha - \bar{z}_{\beta 0}/\bar{p}_\beta)\rangle\mathbf{q}_\beta\} \quad (35)$$

for material 1 in $x_1 < 0$ and

$$\mathbf{U}^{(2)} = \sum_{\beta=1}^{5}\frac{1}{\pi}\mathrm{Im}\{\mathbf{A}^{(2)}\langle \ln(z_\alpha^{*(2)} - z_{\beta 0}^{*(1)})\rangle\mathbf{q}_\beta^{(2)}\}, \quad (36)$$

$$\boldsymbol{\varphi}^{(2)} = \sum_{\beta=1}^{4}\frac{1}{\pi}\mathrm{Im}\{\mathbf{B}^{(2)}\langle \ln(z_\alpha^{*(2)} - z_{\beta 0}^{*(1)})\rangle\mathbf{q}_\beta^{(2)}\} \quad (37)$$

for material 2 in $x_1 > 0$, where $z_{\beta 0}^{*(1)} = z_{\beta 0}^{(1)}/p_\beta^{(1)}$, $z_\alpha^{*(i)} = z_\alpha^{(i)}/p_\alpha^{(i)}$ (i = 1,2). The value of $\mathbf{q}$ is again given in eqn (20), and $\mathbf{q}_\beta^{(1)}, \mathbf{q}_\beta^{(2)}$ are unknown constants which are determined by substituting Eqs. (34)-(37) into Eq. (33). Following the derivation in section in [10], we obtain

$$\mathbf{A}^{(1)}\mathbf{q}_\beta^{(1)} + \overline{\mathbf{A}}^{(2)}\overline{\mathbf{q}}_\beta^{(2)} = \overline{\mathbf{A}}^{(1)}\mathbf{I}_\beta\overline{\mathbf{q}},$$
$$\mathbf{B}^{(1)}\mathbf{q}_\beta^{(1)} + \overline{\mathbf{B}}^{(2)}\overline{\mathbf{q}}_\beta^{(2)} = \overline{\mathbf{B}}^{(1)}\mathbf{I}_\beta\overline{\mathbf{q}}. \quad (38)$$

Solving Eq. (38) yields

$$\mathbf{q}_\beta^{(1)} = \mathbf{B}^{(1)-1}[\mathbf{I} - 2(\mathbf{M}^{(1)-1} + \overline{\mathbf{M}}^{(2)-1})^{-1}\mathbf{L}^{(1)-1}]\overline{\mathbf{B}}^{(1)}\mathbf{I}_\beta\overline{\mathbf{q}}, \quad (39)$$

$$\mathbf{q}_\beta^{(2)} = 2\mathbf{B}^{(2)-1}(\overline{\mathbf{M}}^{(1)-1} + \mathbf{M}^{(2)-1})^{-1}\mathbf{L}^{(1)-1}\mathbf{B}^{(1)}\mathbf{I}_\beta\mathbf{q}, \quad (40)$$

where $\mathbf{M}^{(j)} = -i\mathbf{B}^{(j)}\mathbf{A}^{(j)-1}$ is the surface impedance matrix.

III. Penny-shaped crack problem

III.1 Problem statement and basic equation

Consider a piezoelectric cylinder of radius b containing a centered penny-shaped crack of radius a under axisymmetric electromechanical loads (Fig. 3). For convenience, a cylindrical coordinate system (r, θ, z) originated at the center of the crack is used with the z-axis along the axis of symmetry of the cylinder. The cylinder is assumed to be a transversely isotropic piezoelectric material with the poling direction parallel to the z-axis. It is subjected to the far-field of a normal stress, $\sigma_z = \bar{\sigma}(r)$ and a normal electric displacement, $D_z = \bar{D}(r)$. The constitutive equations are defined in Eqs. (7.1)-(7.6) of Ref. [10]. While the equilibrium equation and the equation of electrostatics for this problem are given as

$$\sigma_{rr,r}+\sigma_{rz,z}+\frac{\sigma_{rr}-\sigma_{\theta\theta}}{r}=0,$$
$$\sigma_{rz,r}+\sigma_{zz,z}+\frac{\sigma_{rz}}{r}=0, \quad (41)$$
$$D_{r,r}+D_{z,z}+\frac{D_r}{r}=0$$

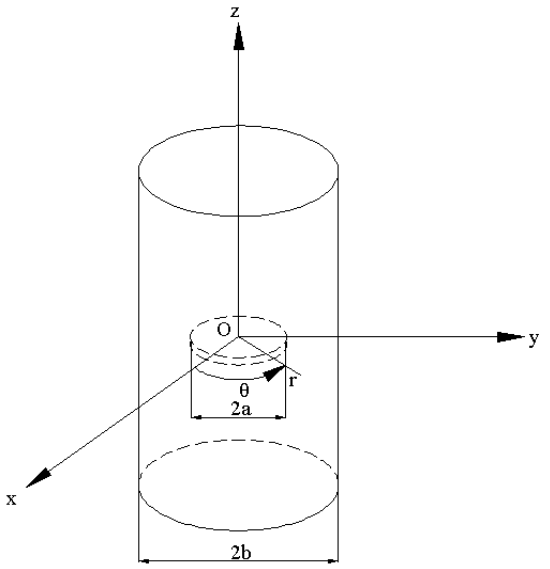

Fig. 3 Penny-shaped crack in a piezoelectric cylinder.

In the derivation of the analytic solution, the following potential functions are introduced [93]

$$u_r=\frac{\partial\Phi}{\partial r}, \quad u_z=k_1\frac{\partial\Phi}{\partial z}, \quad \phi=-k_2\frac{\partial\Phi}{\partial z} \quad (42)$$

where $\Phi(r,z)$ is the potential function, k_1 and k_2 are unknown constants.

Substituting Eq. (42) into the standard governing equation [10], and then into Eq. (41), we have

$$\Phi_{,rr}+\frac{1}{r}\Phi_{,r}+n\Phi_{,zz}=0 \quad (43)$$

where

$$n=\frac{c_{44}+(c_{13}+c_{44})k_1-(e_{31}+e_{15})k_2}{c_{11}}=\frac{c_{33}k_1-e_{33}k_2}{c_{44}k_1+c_{13}+c_{44}-e_{15}k_2}=\frac{e_{33}k_1+\kappa_{33}k_2}{e_{15}k_1+e_{15}+e_{31}+\kappa_{11}k_2} \quad (44)$$

The governing equation (43) becomes

$$\sum_{i=1}^{3}[\Phi_{i,rr}+\frac{1}{r}\Phi_{i,rr}+\Phi_{i,z_iz_i}]$$

or

$$c_{11}\sum_{i=1}^{3}(\frac{\partial\Phi_i}{\partial r^2}+\frac{1}{r}\frac{\partial\Phi_i}{\partial r})+\sum_{i=1}^{3}\{\left[c_{44}+k_{1i}(c_{13}+c_{44})+k_{2i}(e_{31}+e_{15})\right]\frac{\partial\Phi_i}{\partial z^2}\}=0,$$
$$\sum_{i=1}^{3}\{\left[c_{44}k_{1i}+c_{13}+c_{44}+e_{15}k_{2i}\right](\frac{\partial\Phi_i}{\partial r^2}+\frac{1}{r}\frac{\partial\Phi_i}{\partial r})+\left[c_{33}k_{1i}+e_{33}k_{2i}\right]\frac{\partial\Phi_i}{\partial z^2}\}=0,$$
$$\sum_{i=1}^{3}\{\left[e_{15}k_{1i}+e_{31}+e_{15}-d_{11}k_{2i}\right](\frac{\partial\Phi_i}{\partial r^2}+\frac{1}{r}\frac{\partial\Phi_i}{\partial r})+\left[e_{33}k_{1i}-d_{33}k_{2i}\right]\frac{\partial\Phi_i}{\partial z^2}\}=0 \quad (45)$$

where $z_i=z/\sqrt{n_i}=\mu_i z$, μ_i are the roots of Eq (2.8) presented in [10] and $\Phi_i(r,z)$ $(i=1,2,3)$ are the corresponding potential functions. According to the principle of superposition, the displacement and electric potential equations become

$$u_r=\sum_{1}^{3}\frac{\partial\Phi_i}{\partial r}, \quad u_z=\sum_{i=1}^{3}k_{1i}\frac{\partial\Phi_i}{\partial z}, \quad \phi=-\sum_{i=1}^{3}k_{2i}\frac{\partial\Phi_i}{\partial z} \quad (46)$$

where k_{1i} and k_{2i} $(i=1,2,3)$ are determined from Eq. (44).

Following the way presented in [94], we take the solution of the Eq. (45) in the form:

$$\Phi_i(r,z)=\int_0^\infty\frac{1}{\xi}\left[A_i(\xi)I_0(\frac{\xi r}{\mu_i})\cos(\xi z)+B_i(\xi)\exp(-\xi\mu_i z)J_0(\xi r)\right]d\xi \quad (47)$$

where $A_i(\xi)$, $B_i(\xi)$, $(i=1,2,3)$ are the unknown functions to be determined.

Then we have the expressions of components of displacement, stress and electric displacement in the following form:

$$u_z(r,z)=-\sum_{i=1}^{3}k_{1i}\int_0^\infty A_i(\xi)I_0(\frac{\xi r}{\mu_i})\sin(\xi z)d\xi-\sum_{i=1}^{3}k_{1i}s_i\int_0^\infty B_i(\xi)J_0(\xi r)e^{-\xi\mu_i z}d\xi+\bar{a}(r)z \quad (48)$$

$$u_r(r,z)=\sum_{i=1}^{3}\frac{1}{\mu_i}\int_0^\infty A_i(\xi)I_1(\frac{\xi r}{\mu_i})\cos(\xi z)d\xi-\sum_{i=1}^{3}\int_0^\infty B_i(\xi)J_1(\xi r)e^{-\xi\mu_i z}d\xi \quad (49)$$

$$\varphi(r,z)=\sum_{i=1}^{3}k_{2i}\int_0^\infty A_i(\xi)I_1(\frac{\xi r}{\mu_i})\sin(\xi z)d\xi+\sum_{i=1}^{3}k_{2i}s_i\int_0^\infty B_i(\xi)J_0(\xi r)e^{-\xi\mu_i z}d\xi-\bar{b}(r)z \quad (50)$$

$$\sigma_z=-\sum_{i=1}^{3}\frac{F_{1i}}{\mu_i^2}\int_0^\infty\xi A_i(\xi)I_0(\frac{\xi r}{\mu_i})\cos(\xi z)d\xi+\sum_{i=1}^{3}F_{1i}\int_0^\infty\xi B_i(\xi)J_0(\xi r)e^{-\xi\mu_i z}d\xi+\bar{c}(r) \quad (51)$$

$$\sigma_r=-\sum_{i=1}^{3}\frac{F_{5i}}{\mu_i^2}\int_0^\infty\xi A_i(\xi)I_0(\frac{\xi r}{\mu_i})\cos(\xi z)d\xi+\frac{c_{11}-c_{12}}{2}\sum_{i=1}^{3}\frac{1}{\mu_i^2}\int_0^\infty\xi A_i(\xi)I_2(\frac{\xi r}{\mu_i})\cos(\xi z)d\xi+\sum_{i=1}^{3}F_{5i}\int_0^\infty\xi B_i(\xi)J_0(\xi r)e^{-\xi\mu_i z}d\xi+\frac{c_{11}-c_{12}}{2}\sum_{i=1}^{3}\int_0^\infty\xi B_i(\xi)J_2(\xi r)e^{-\xi\mu_i z}d\xi \quad (52)$$

$$\sigma_{zr}=-\sum_{i=1}^{3}\frac{F_{3i}}{\mu_i^2}\int_0^\infty\xi A_i(\xi)I_1(\frac{\xi r}{\mu_i})\sin(\xi z)d\xi+\sum_{i=1}^{3}F_{3i}\int_0^\infty\xi B_i(\xi)J_1(\xi r)e^{-\xi\mu_i z}d\xi \quad (53)$$

$$D_z = -\sum_{i=1}^{3} \frac{F_{2i}}{\mu_i^2} \int_0^\infty \xi A_i(\xi) I_0\left(\frac{\xi r}{\mu_i}\right) \cos(\xi z) d\xi + \sum_{i=1}^{3} F_{2i} \int_0^\infty \xi B_i(\xi) J_0(\xi r) e^{-\xi \mu_i z} d\xi + \bar{d}(r) \quad (54)$$

$$D_r = -\sum_{i=1}^{3} \frac{F_{4i}}{\mu_i^2} \int_0^\infty \xi A_i(\xi) I_1\left(\frac{\xi r}{\mu_i}\right) \sin(\xi z) d\xi + \sum_{i=1}^{3} F_{4i} \int_0^\infty \xi B_i(\xi) J_1(\xi r) e^{-\xi \mu_i z} d\xi \quad (55)$$

where

$$F_{1i} = (c_{33}k_{1i} - e_{33}k_{2i})\mu_i^2 - c_{13}, \quad F_{2i} = (e_{33}k_{1i} + d_{33}k_{2i})\mu_i^2 - e_{31},$$
$$F_{3i} = \left[c_{44}(1+k_{1i}) - e_{15}k_{2i}\right]\mu_i, \quad F_{4i} = \left[e_{15}(1+k_{1i}) + d_{11}k_{2i}\right]\mu_i,$$
$$F_{5i} = (c_{13}k_{1i} - e_{31}k_{2i})\mu_i^2 - \frac{c_{11}+c_{12}}{2}$$
$$\bar{a}(r) = \frac{d_{33}\bar{\sigma}(r) + \bar{e}_{33}\bar{D}(r)}{c_{33}d_{33} + e_{33}^2}, \quad \bar{b}(r) = \frac{c_{33}\bar{D}(r) - e_{33}\bar{\sigma}(r)}{c_{33}d_{33} + e_{33}^2}, \quad (56)$$
$$\bar{c}(r) = \bar{\sigma}(r), \quad \bar{d}(r) = \bar{D}(r)$$

III.2 Derivation of integral equations

In the derivation, we will consider separately two sets of boundary conditions.

Case (i): In the first case it is assumed that the piezoelectric cylindrical surface is free from shear and is supported in such a way that the radial component of the displacement vector vanishes on the surface. Such a situation would arise physically if the piezoelectric cylinder was embedded in a rigid cylindrical hollow (of exactly the same radius) and was then deformed by the application of a known stress and an electric displacement at the end of the piezoelectric cylinder. The problem of determining the distribution of stress and electric displacement in the vicinity of the crack is equivalent to that of finding the distribution of stress and electric displacement in the semi-infinite cylinder $z \geq 0$, $0 \leq r \leq a$,when its plane boundary $z = 0$ is subjected to the condition:

$$\begin{aligned} &\sigma_z(r,0) = 0, \quad D_z(r,0^+) = D_z(r,0^-), \\ &E_r(r,0^+) = E_r(r,0^+), \quad (0 \leq r < a); \\ &u_z(r,0) = 0, \quad \phi(r,0) = 0, \quad (a < r < b); \\ &\sigma_{rz}(r,0) = 0, \quad (0 \leq r < b) \end{aligned} \quad (57)$$

and its curved boundary $r = b$ is subjected to the conditions:

$$u_r(b,z) = 0, \quad \sigma_{rz}(b,z) = 0, \quad D_r(b,z) = 0 \quad (58)$$

From the boundary conditions (57) and (58) and making use of the Fourier inversion theorem and the Hankel inversion theorem we find that:

$$A_1(\xi) = \frac{1}{\Delta(\xi)} f_1(\xi) \sum_{i=1}^{3} N_{1i}(\xi), \quad A_2(\xi) = \frac{1}{\Delta(\xi)} f_2(\xi) \sum_{i=1}^{3} N_{2i}(\xi), \quad A_3(\xi) = \frac{1}{\Delta(\xi)} f_3(\xi) \sum_{i=1}^{3} N_{3i}(\xi) \quad (59)$$

$$B_1(\xi) = M_1 B_1(\xi), \quad B_2(\xi) = M_2 B_1(\xi), \quad B_3(\xi) = M_3 B_1(\xi) \quad (60)$$

in which

$$M_1 = 1, \quad M_2 = \frac{F_{31}k_{23}\mu_3 - F_{33}k_{21}\mu_1}{F_{33}k_{22}\mu_2 - F_{32}k_{23}\mu_3}, \quad M_3 = \frac{F_{32}k_{21}\mu_1 - F_{31}k_{22}\mu_2}{F_{33}k_{22}\mu_2 - F_{32}k_{23}\mu_3}$$

$$f_i(\xi) = \frac{2}{\pi} \int_0^\infty \frac{\eta B_1(\eta) J_1(\eta b)}{\eta^2 s_i^2 + \xi^2} d\eta \quad (61)$$

,

$$\begin{aligned} \Delta(\xi) &= \left[h_{12}(\xi)h_{33}(\xi) - h_{32}(\xi)h_{13}(\xi)\right]h_{21}(\xi) \\ &+ \left[h_{31}(\xi)h_{13}(\xi) - h_{11}(\xi)h_{33}(\xi)\right]h_{22}(\xi) \\ &+ \left[h_{11}(\xi)h_{32}(\xi) - h_{31}(\xi)h_{12}(\xi)\right]h_{23}(\xi), \\ N_{1i}(\xi) &= \left[(h_{13}(\xi)h_{22}(\xi) - h_{12}(\xi)h_{23}(\xi)\right]g_{3i} \\ &+ \left[(h_{12}(\xi)h_{33}(\xi) - h_{13}(\xi)h_{32}(\xi)\right]g_{2i} \\ &+ \left[(h_{23}(\xi)h_{32}(\xi) - h_{22}(\xi)h_{33}(\xi)\right]g_{1i}, \\ N_{2i}(\xi) &= \left[(h_{11}(\xi)h_{23}(\xi) - h_{21}(\xi)h_{13}(\xi)\right]g_{3i} \\ &+ \left[(h_{13}(\xi)h_{31}(\xi) - h_{11}(\xi)h_{33}(\xi)\right]g_{2i} \\ &+ \left[(h_{21}(\xi)h_{33}(\xi) - h_{31}(\xi)h_{23}(\xi)\right]g_{1i}, \\ N_{3i}(\xi) &= \left[(h_{12}(\xi)h_{21}(\xi) - h_{11}(\xi)h_{22}(\xi)\right]g_{3i} \\ &+ \left[(h_{11}(\xi)h_{32}(\xi) - h_{31}(\xi)h_{12}(\xi)\right]g_{2i} \\ &+ \left[(h_{22}(\xi)h_{31}(\xi) - h_{21}(\xi)h_{32}(\xi)\right]g_{1i}, \end{aligned}$$

with

$$h_{1i}(\xi) = \frac{F_{4i}}{s_i^2} I_1\left(\frac{\xi b}{s_i}\right), \quad g_{1i} = F_{4i}M_i,$$
$$h_{2i}(\xi) = \frac{F_{3i}}{s_i^2} I_1\left(\frac{\xi b}{s_i}\right), \quad g_{2i} = F_{3i}M_i s_i,$$
$$h_{3i}(\xi) = \frac{1}{s_i} I_1\left(\frac{\xi b}{s_i}\right), \quad g_{3i} = M_i s_i. \quad (62)$$

From Eqs. (57) and (58), we can obtain a system of dual integral equation:

$$-\int_0^\infty \xi \left[\frac{F_{11}}{s_1^2} I_0\left(\frac{\xi r}{s_1}\right) A_1(\xi) + \frac{F_{12}}{s_2^2} I_0\left(\frac{\xi r}{s_2}\right) A_2(\xi) + \frac{F_{13}}{s_3^2} I_0\left(\frac{\xi r}{s_3}\right) A_3(\xi)\right] d\xi$$
$$+ \int_0^\infty \xi \left[M_1 F_{11} + M_2 F_{12} + M_3 F_{13}\right] B_1(\xi) J_0(\xi r) d\xi = -\bar{c}(r), \quad (0 \leq r < a), \quad (63)$$

$$\int_0^\infty \left[M_1 k_{11} s_1 + M_2 k_{12} s_2 + M_3 k_{13} s_3\right] B_1(\xi) J_0(\xi r) d\xi = 0 \quad (a < r < b) \quad (64)$$

This equation can be solved by using the function $\psi(\alpha)$ defined by

$$B_1(\xi) = \int_0^a \psi(\alpha) \sin(\xi\alpha) d\alpha \quad (65)$$

where $\psi(0) = 0$.

Using solutions of integrals given in page 274 of [10], we can obtain a Fredholm integral equation of the second kind in the following form,

$$\psi(\alpha)+\int_0^a \psi(\beta)L(\alpha,\beta)d\beta=\frac{2}{\pi m_0}\int_0^\alpha \frac{r\bar{c}(r)}{\sqrt{\alpha^2-r^2}}dr \tag{66}$$

in which

$$L(\alpha,\beta)=\frac{4}{\pi^2 m_0}\sum_{j=1}^{3}\frac{F_{1j}}{s_j}\int_0^\infty \frac{1}{\Delta(\xi)}\sinh(\frac{\xi\alpha}{s_j}) \times\sum_{i=1}^{3}\frac{1}{s_i^2}N_{ji}(\xi)\sinh(\frac{\xi\beta}{s_i})K_1(\frac{\xi b}{s_i})d\xi \tag{67}$$

case (ii): In the second case we assume that the piezoelectric cylindrical surface is stress free. The conditions (57) remain the same as in case (i), and the boundary conditions (58) are replaced by the following conditions:

$$\sigma_{rr}(b,z)=0,\ \ \sigma_{rz}(b,z)=0\,,\ \ D_r(b,z)=0\,,\ \ (z\ge 0)$$

Conducting the procedure similar to that in case (i), we can have:

$$A_1(\xi)=\frac{1}{\Delta(\xi)}\sum_{i=1}^{3}\left[N_{1i}(\xi)f_{1i}(\xi)+P_{1i}(\xi)f_{2i}(\xi)+W_{1i}(\xi)f_{3i}(\xi)\right],$$
$$A_2(\xi)=\frac{1}{\Delta(\xi)}\sum_{i=1}^{3}\left[N_{2i}(\xi)f_{1i}(\xi)+P_{2i}(\xi)f_{2i}(\xi)+W_{2i}(\xi)f_{3i}(\xi)\right],$$
$$A_3(\xi)=\frac{1}{\Delta(\xi)}\sum_{i=1}^{3}\left[N_{3i}(\xi)f_{1i}(\xi)+P_{3i}(\xi)f_{2i}(\xi)+w_{3i}(\xi)f_{3i}(\xi)\right]. \tag{68}$$

in which

$$f_{2i}(\xi)=\frac{2}{\pi}\int_0^\infty \frac{\eta^2 B_1(\eta)J_0(\eta b)}{\eta^2 s_i^2+\xi^2}d\eta,$$

$$f_{3i}(\xi)=\frac{2}{\pi}\int_0^\infty \frac{\eta^2 B_1(\eta)J_2(\eta b)}{\eta^2 s_i^2+\xi^2}d\eta\,,$$

$$N_{1i}(\xi)=\left[h_{52}(\xi)-h_{42}(\xi)\right]\left[h_{33}(\xi)g_{2i}-h_{23}(\xi)g_{3i}\right] +\left[h_{53}(\xi)-h_{43}(\xi)\right]\left[h_{22}(\xi)g_{3i}-h_{32}(\xi)g_{2i}\right],$$

$$P_{1i}(\xi)=\frac{1}{\xi}\left[h_{23}(\xi)h_{32}(\xi)-h_{22}(\xi)h_{33}(\xi)\right]g_{5i}\,,$$

$$W_{1i}(\xi)=\frac{1}{\xi}\left[h_{23}(\xi)h_{32}(\xi)-h_{22}(\xi)h_{33}(\xi)\right]g_{4i}\,,$$

$$N_{2i}(\xi)=\left[h_{53}(\xi)-h_{43}(\xi)\right]\left[h_{31}(\xi)g_{2i}-h_{21}(\xi)g_{3i}\right] +\left[h_{51}(\xi)-h_{41}(\xi)\right]\left[h_{23}(\xi)g_{3i}-h_{33}(\xi)g_{2i}\right],$$

$$P_{2i}(\xi)=\frac{1}{\xi}\left[h_{21}(\xi)h_{33}(\xi)-h_{23}(\xi)h_{31}(\xi)\right]g_{5i}\,,$$

$$W_{2i}(\xi)=\frac{1}{\xi}\left[h_{21}(\xi)h_{33}(\xi)-h_{23}(\xi)h_{31}(\xi)\right]g_{4i}$$

$$N_{3i}(\xi)=\left[h_{51}(\xi)-h_{41}(\xi)\right]\left[h_{32}(\xi)g_{2i}-h_{22}(\xi)g_{3i}\right] +\left[h_{52}(\xi)-h_{42}(\xi)\right]\left[h_{21}(\xi)g_{3i}-h_{31}(\xi)g_{2i}\right],$$

$$P_{3i}(\xi)=\frac{1}{\xi}\left[h_{22}(\xi)h_{31}(\xi)-h_{21}(\xi)h_{32}(\xi)\right]g_{5i}\,,$$

$$W_{3i}(\xi)=\frac{1}{\xi}\left[h_{22}(\xi)h_{31}(\xi)-h_{21}(\xi)h_{32}(\xi)\right]g_{4i}$$

$$\Delta(\xi)=\left\{\begin{matrix}\left[-h_{53}(\xi)+h_{43}(\xi)\right]h_{32}(\xi)\\ +\left[h_{52}(\xi)-h_{42}(\xi)\right]h_{33}(\xi)\end{matrix}\right\}h_{21}(\xi)$$
$$+\left\{\left[h_{53}(\xi)-h_{43}(\xi)\right]h_{31}(\xi)+\left[-h_{51}(\xi)+h_{41}(\xi)\right]h_{33}(\xi)\right\}h_{22}(\xi)$$
$$+\left\{\left[h_{51}(\xi)-h_{41}(\xi)\right]h_{32}(\xi)+\left[-h_{52}(\xi)+h_{42}(\xi)\right]h_{31}(\xi)\right\}h_{23}(\xi)$$

with

$$h_{1i}(\xi)=\frac{F_{4i}}{s_i^2}I_1(\frac{\xi b}{s_i})\,,\ \ g_{1i}=F_{4i}M_i\,,$$

$$h_{2i}(\xi)=\frac{F_{3i}}{s_i^2}I_1(\frac{\xi b}{s_i})\,,\ \ g_{2i}=F_{3i}M_i s_i\,,$$

$$h_{3i}(\xi)=\frac{1}{s_i}I_1(\frac{\xi b}{s_i})\,,\ \ g_{3i}=M_i s_i\,,$$

$$h_{4i}(\xi)=\frac{c_{11}-c_{12}}{2}\frac{1}{s_i^2}I_2(\frac{\xi b}{s_i})\,,\ \ g_{4i}=\frac{c_{11}-c_{12}}{2}M_i s_i\,,$$

$$h_{5i}(\xi)=\frac{F_{5i}}{s_i^2}I_0(\frac{\xi b}{s_i})\,,\ \ g_{5i}=F_{5i}M_i s_i\,. \tag{69}$$

and $B_i(i=2,3)$, $f_{1i}(\xi)$ are the same to that in case(i).

Then we can obtain a Fredholm integral equation of the second kind which is exactly the same as that given in Eqs. (63) and (64), except the kernel $L(\alpha,\beta)$ takes the following form.

$$L(\alpha,\beta)=\frac{4}{\pi^2 m_0}\sum_{j=1}^{3}\frac{F_{1j}}{s_j}\int_0^\infty \frac{1}{\Delta(\xi)}\sinh(\frac{\xi\alpha}{s_j})\sum_{i=1}^{3}\frac{1}{s_i^2}\sinh(\frac{\xi\beta}{s_i}) \times\left\{N_{ji}(\xi)K_1(\frac{\xi b}{s_i})-\frac{\xi}{s_i}P_{ji}(\xi)K_0(\frac{\xi b}{s_i}) +\frac{\xi}{s_i}W_{ji}(\xi)K_2(\frac{\xi b}{s_i})\right\}d\xi \tag{70}$$

Each kind of the field intensity factors is obtained in the form

$$K^\sigma=K_I=\lim_{r\to a^+}\sqrt{2\pi(r-a)}\sigma_z(r,0)=\sqrt{\frac{\pi}{a}}m_0\psi(a)\,,$$

$$K^D=\lim_{r\to a^+}\sqrt{2\pi(r-a)}D_z(r,0)=\sqrt{\frac{\pi}{a}}m_1\psi(a)\,,$$

$$K^{\varepsilon} = \lim_{r\to a^+}\sqrt{2\pi(r-a)}\varepsilon_z(r,0) = \sqrt{\frac{\pi}{a}}m_2\psi(a),$$

$$K^{E} = \lim_{r\to a^+}\sqrt{2\pi(r-a)}E_z(r,0) = \sqrt{\frac{\pi}{a}}m_3\psi(a) \quad (71)$$

in which

$$m_0 = -(M_1F_{11} + M_2F_{12} + M_3F_{13}),$$
$$m_1 = -(F_{21}M_1 + F_{22}M_2 + F_{23}M_3),$$
$$m_2 = -(k_{11}s_1^2M_1 + k_{12}s_1^2M_2 + k_{13}s_1^3M_3),$$
$$m_3 = -(k_{21}s_1^2M_1 + k_{22}s_2^2M_2 + k_{23}s_3^2M_3) \quad (72)$$

and K^{σ}, K^{D}, K^{ε} and K^{E} are the stress intensity factor, electric displacement intensity factor, strain intensity factor and electric field intensity factor, respectively.

IV. Boundary elements for piezoelectric materials

IV.1 Green functions for a hole embedded in an infinite piezoelectric solid

Consider a hole embedded in an infinite piezoelectric solid subjected to a line temperature discontinuity located at a point (x_{10}, x_{20}). Green functions for such a problem have been given in [45]. They are:

$$T = 2\,\mathrm{Re}[g'(z_t)] = 2\,\mathrm{Re}[f_0(\zeta_t) + f_1(\zeta_t)] \quad (73)$$

$$\vartheta = -2\,\mathrm{Re}[ikg'(z_t)] = -2\,\mathrm{Re}[ikf_0(\zeta_t) + ikf_1(\zeta_t)] \quad (74)$$

$$\mathbf{u} = 2\,\mathrm{Re}\{-\mathbf{A}[\mathbf{F}_1(\boldsymbol{\zeta}) + \mathbf{F}_2(\boldsymbol{\zeta})\mathbf{P}^{-1}\bar{\tau}]\mathbf{B}^{-1}\bar{\mathbf{d}} + \mathbf{c}g(\zeta_t)\} \quad (75)$$

$$\boldsymbol{\phi} = 2\,\mathrm{Re}\{-\mathbf{B}[\mathbf{F}_1(\boldsymbol{\zeta}) + \mathbf{F}_2(\boldsymbol{\zeta})\mathbf{P}^{-1}\bar{\tau}]\mathbf{B}^{-1}\bar{\mathbf{d}} + \mathbf{d}g(\zeta_t)\} \quad (76)$$

where T, ϑ, $\mathbf{u}$ and $\boldsymbol{\phi}$ represent temperature, heat-flow function, EDEP and SED function vectors, respectively. $i=\sqrt{-1}$, "Re" represents the real part of a complex number, $\boldsymbol{\zeta} = \{\zeta_1\ \zeta_2\ \zeta_3\ \zeta_4\}^T$, $\mathbf{P}$ = diag [p_1 p_2 p_3 p_4], τ and p_k are heat and electro-elastic eigen values of the materials whose imaginary parts are positive. $k = \sqrt{k_{11}k_{22} - k_{12}^2}$, where k_{ij} is the thermal conductivity, **A**, **B**, **c** and **d** are the material eigenvector matrices and vectors which are defined in the literature (see [10], for example). ζ_k and ζ_t are related to the complex variables $z_k\,(= x_1 + p_k x_2)$ and $z_t\,(= x_1 + \tau x_2)$ by, respectively

$$z_k = a(a_{1k}\zeta_k + a_{2k}\zeta_k^{-1} + e_{n1}a_{3k}\zeta_k^{n} + e_{n1}a_{4k}\zeta_k^{-n}) \quad (77)$$

$$z_t = a(a_{1\tau}\zeta_t + a_{2\tau}\zeta_t^{-1} + e_{n1}a_{3\tau}\zeta_t^{n} + e_{n1}a_{4\tau}\zeta_t^{-n}) \quad (78)$$

in which

$$a_{1k} = (1 - ip_k e)/2,\ a_{2k} = (1 + ip_k e)/2,$$
$$a_{3k} = \gamma(1 + ip_k e)/2,\ a_{4k} = \gamma(1 - ip_k e)/2 \quad (79)$$

$$a_{1\tau} = (1 - i\tau e)/2,\ a_{2\tau} = (1 + i\tau e)/2$$
$$a_{3\tau} = \gamma(1 + i\tau e)/2,\ a_{4\tau} = \gamma(1 - i\tau e)/2 \quad (8)$$

where $e_{ij} = 1$ if $i \neq j$; $e_{ij} = 0$ if $i = j$, $0 < e \le 1$, n is an integer and has the same value for both subscript and argument of the functions. γ and a are real parameters. By an appropriate selection of the parameters e, n and γ, we can obtain various kinds of cavities or holes, such as ellipse (n=1), circle (n=e=1), triangular (n=2), square (n=3) and pentagon (n=4). The functions f_0, f_1, $\mathbf{F}_1$, $\mathbf{F}_2$ and g_t can be found in [8]. With the above solutions, the heat flow h_i and SED $\boldsymbol{\Pi}_i$ ($= \{\sigma_{1i}\ \sigma_{2i}\ \sigma_{3i}\ D_i\}^T$) are calculated by the relations:

$$h_1 = -\vartheta_{,2},\quad h_2 = \vartheta_{,1},\quad \boldsymbol{\Pi}_1 = -\boldsymbol{\phi}_{,2},\quad \boldsymbol{\Pi}_2 = \boldsymbol{\phi}_{,1} \quad (80)$$

where h_i, σ_{ij} and D_i are, respectively, heat flow, stress and electric displacement.

IV.2 BEM for thermopiezoelectric problem

Consider again a 2D thermopiezoelectric solid inside of which there exist a hole and a number of cracks with arbitrary orientation and size. The numerical approach to such a problem usually involves the following steps. (i) Solve a heat transfer problem first to obtain the steady-state T field. (ii) Calculate the electroelastic field caused by the T field, then plus an isothermal solution to satisfy the corresponding mechanical boundary conditions. (iii) Finally, solve the modified problem for electroelastic fields. In what follows, we begin by deriving the variational principle for temperature discontinuity and then extend it to the case of thermo-electroelasticity.

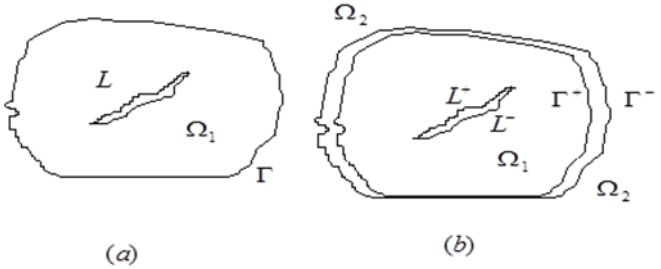

Fig. 4 Configuration of the plate

IV.2.1 BEM for temperature discontinuity problem

Let us consider a finite region Ω_1 bounded by $\Gamma(= \Gamma_h + \Gamma_T)$, as shown in Fig. 4(a). The heat transfer problem to be considered is stated as:

$$k_{ij}T_{,ij} = 0 \qquad \text{in } \Omega_1 \quad (81)$$

$$h_n = h_i n_i = h_0 \qquad \text{on } \Gamma_h \quad (82)$$

$$T = T_0 \qquad \text{on } \Gamma_T \quad (83)$$

$$h_i n_i = 0 \qquad \text{on } L \quad (84)$$

where n_i is the normal to the boundary Γ, h_0 and T_0 are the prescribed values of heat flow and temperature, which act on the boundaries Γ_h and Γ_T, respectively. For simplicity, we define $\hat{T} = T\big|_{L^+} - T\big|_{L^-}$ on L ($=L^+ + L^-$), where $\hat{T}$ is the temperature discontinuity, L is the union of all cracks, L^+ and L^- are defined in Fig. 4(b). It should be pointed out that the boundary condition along the hole is automatically satisfied due to the use of the Green function given in Eqs. (73) and (74) . Naturally, the hole boundary condition is not involved in the following analysis.

Further, if we let Ω_2 be the complementary region of Ω_1 (i.e., the union of Ω_1 and Ω_2 forms the infinite region Ω) and $\hat{T} = T\big|_{\Gamma^+} - T\big|_{\Gamma^-} = T_0$, the problem shown in Fig 4(a) can be extended to the infinite case (see Fig. 4b). Here $\Gamma = \Gamma^+ + \Gamma^-$, where Γ^+ and Γ^- stand for the boundaries of Ω_1 and Ω_2, respectively [see Fig. 4(b)]. In a way similar to that in [8], the total generalised potential energy for the thermal problem defined above is given by:

$$P(T,\hat{T}) = \frac{1}{2}\int_\Omega k_{ij}T_{,i}T_{,j}\,d\Omega + \int_\Gamma h_n\hat{T}\,dL \tag{85}$$

By transforming the area integral in Eq. (85) to a boundary integral, we have

$$P(T,\hat{T}) = -\frac{1}{2}\int_L \vartheta(T)\hat{T}_{,s}\,ds + \int_\Gamma h_n\hat{T}\,ds \tag{86}$$

in which the relation

$$h_i = -k_{ij}T_{,j} \text{ and } \int_L h_n\hat{T}ds = \int_L[(\vartheta\hat{T})_{,s} - \vartheta\hat{T}_{,s}]ds \tag{87}$$

and the temperature discontinuity is assumed to be continuous over L and zero at the ends of L. Moreover, temperature T in Eq. (86) can be expressed in terms of $\hat{T}$ through use of Eq. (73). Therefore, the potential energy can be further written as

$$P(\hat{T}) = -\frac{1}{2}\int_L \vartheta(\hat{T})\hat{T}_{,s}\,ds + \int_\Gamma h_n\hat{T}\,ds \tag{88}$$

The analytical results for the minimum of potential (88) is not, in general, possible, and therefore a numerical procedure must be used to solve the problem. As in conventional BEM, the boundaries Γ and L are divided into a series of linear boundary elements for which the temperature discontinuity may be approximated by a linear function. To illustrate this, take a particular element m, which is a line connected by nodes m and m+1, as an example (see Fig. 5)

$$\hat{T}(s) = \hat{T}_m F_m(s) + \hat{T}_{m+1}F_{m+1}(s) \tag{89}$$

where $\hat{T}_m$ is the temperature discontinuity at node m, and functions $F_m(s)$, $F_{m+1}(s)$ are shown in Figure 5.

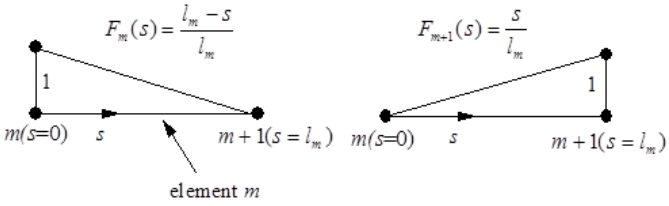

Fig. 5 The definitions of $F_m(s)$ and $F_{m+1}(s)$

On the use of Eqs. (73), (74) and (89), the temperature and heat-flux function at point z_t are

$$T(z_t) = \sum_{m=1}^{M} \mathrm{Im}[a_m(z_t)]\hat{T}_m \tag{90}$$

$$\vartheta(z_t) = -k\sum_{m=1}^{M} \mathrm{Re}[a_m(z_t)]\hat{T}_m \tag{91}$$

where M is the total number of nodes, "Im" represents the imaginary part of a complex number, and

$$a_m(\zeta_t) = \frac{1}{2\pi}\int_{l_{m-1}} \{\ln(\zeta_t - \zeta_{t0}^{m-1}) + \ln(\zeta_t^{-1} - \bar{\zeta}_{t0}^{m-1})\}\frac{l_{m-1}-s}{l_{m-1}}ds + \frac{1}{2\pi}\int_{l_m} \{\ln(\zeta_t - \zeta_{t0}^{m}) + \ln(\zeta_t^{-1} - \bar{\zeta}_{t0}^{m})\}\frac{s}{l_m}ds \tag{92}$$

in which ζ_{t0} can be expressed in terms of s by the relations

$$z_t = f(\zeta_t) = a(a_{1\tau}\zeta_t + a_{2\tau}\zeta_t^{-1} + e_{n1}a_{3\tau}\zeta_t^n + e_{n1}a_{4\tau}\zeta_t^{-n}), \tag{93}$$

$$\zeta_{t0}^{m-1} = f^{-1}(z_{t0}^{m-1}), \qquad \zeta_{t0}^{m} = f^{-1}(z_{t0}^{m}), \tag{94}$$

$$z_{t0}^{m-1} = d_m + s(\cos\alpha_{m-1} + \tau\sin\alpha_{m-1}),$$
$$z_{t0}^{m} = d_m + s(\cos\alpha_m + \tau\sin\alpha_m) \tag{95}$$

and $d_m = x_{1m} + \tau x_{2m}$, (x_{1m}, x_{2m}) is the coordinates at node m, α_m is the angle between the element m and x_1-axis, α_{m-1} is defined similarly. It should be pointed out that the solution of ζ_{t0} in Eq. (94) is multi-valued, as there exist n-roots located outside the unit circle [46]. The root whose magnitude has a minimum value is chosen in our analysis [46].

Using Eq. (90), the temperature at node j can be written as

$$T_j(\zeta_{tj}) = \sum_{m=1}^{M} \mathrm{Im}[a_m(\zeta_{tj})]\hat{T}_m \tag{96}$$

Substituting Eq. (89) into Eq. (88) yields

$$P(\hat{T}) \approx \sum_{j=1}^{M}[\sum_{m=1}^{M}(-\frac{1}{2}K_{mj}\hat{T}_m\hat{T}_j) + G_j\hat{T}_j] \tag{97}$$

where K_{mj} is known as the stiffness matrix and G_j the

equivalent nodal heat flux vector, which are given by:

$$K_{mj} = -\frac{k}{l_{j-1}}\int_{l_{j-1}} \mathrm{Re}[a_m(\zeta_{t0}^{j-1})]ds + \frac{k}{l_j}\int_{l_j} \mathrm{Re}[a_m(\zeta_{t0}^{j})]ds \quad (98)$$

$$G_j = \int_{l_{j-1}+l_j} h_{*0}F_j(s)ds \quad (99)$$

The minimization of $P(\hat{T})$ yields

$$\sum_{j=1}^{M} K_{mj}\hat{T}_j = G_m \quad (100)$$

The final form of the linear equations to be solved is obtained by selecting the appropriate ones, from among Eqs. (96) and (100). Eq. (96) will be chosen for those nodes at which the temperature is prescribed, and Eq. (100) for the remaining nodes. After the nodal temperature discontinuities have been calculated, the EDEP and SED at any point in the region can be evaluated by using Eqs. (75), (76) and (80). They are

$$\mathbf{u} = \sum_{j=1}^{M}\mathbf{w}_j\hat{T}_j,\ \boldsymbol{\Pi}_1 = \sum_{j=1}^{M}\mathbf{x}_j\hat{T}_j,\ \boldsymbol{\Pi}_2 = \sum_{j=1}^{M}\mathbf{y}_j\hat{T}_j \quad (101)$$

where

$$\mathbf{w}_j = -\frac{1}{2\pi}\mathrm{Im}\{\int_{l_{j-1}}[\mathbf{A}(\mathbf{F}_1(\boldsymbol{\zeta})+\mathbf{F}_2(\boldsymbol{\zeta})\mathbf{P}^{-1}\bar{\tau})\mathbf{B}^{-1}\bar{\mathbf{d}} - \mathbf{c}g(\zeta_t)]\frac{l_{j-1}-s}{l_{j-1}}ds\}$$
$$-\frac{1}{2\pi}\mathrm{Im}\{\int_{l_j}[\mathbf{A}(\mathbf{F}_1(\boldsymbol{\zeta})+\mathbf{F}_2(\boldsymbol{\zeta})\mathbf{P}^{-1}\bar{\tau})\mathbf{B}^{-1}\bar{\mathbf{d}} - \mathbf{c}g(\zeta_t)]\frac{s}{l_j}ds\} \quad (102)$$

$$\mathbf{x}_j = \frac{1}{2\pi}\mathrm{Im}\{\int_{l_{j-1}}[\mathbf{B}(\mathbf{F}_1'(\boldsymbol{\zeta})\mathbf{P}+\mathbf{F}_2'(\boldsymbol{\zeta})\bar{\tau})\mathbf{B}^{-1}\bar{\mathbf{d}} - \mathbf{c}\tau g'(\zeta_t)]\frac{l_{j-1}-s}{l_{j-1}}ds\}$$
$$+\frac{1}{2\pi}\mathrm{Im}\{\int_{l_j}[\mathbf{B}(\mathbf{F}_1'(\boldsymbol{\zeta})\mathbf{P}+\mathbf{F}_2'(\boldsymbol{\zeta})\bar{\tau})\mathbf{B}^{-1}\bar{\mathbf{d}} - \mathbf{c}\tau g'(\zeta_t)]\frac{s}{l_j}ds\} \quad (103)$$

$$\mathbf{y}_j = -\frac{1}{2\pi}\mathrm{Im}\{\int_{l_{j-1}}[\mathbf{B}(\mathbf{F}_1'(\boldsymbol{\zeta})+\mathbf{F}_2'(\boldsymbol{\zeta})\mathbf{P}^{-1}\bar{\tau})\mathbf{B}^{-1}\bar{\mathbf{d}} - \mathbf{c}g'(\zeta_t)]\frac{l_{j-1}-s}{l_{j-1}}ds\}$$
$$-\frac{1}{2\pi}\mathrm{Im}\{\int_{l_j}[\mathbf{B}(\mathbf{F}_1'(\boldsymbol{\zeta})+\mathbf{F}_2'(\boldsymbol{\zeta})\mathbf{P}^{-1}\bar{\tau})\mathbf{B}^{-1}\bar{\mathbf{d}} - \mathbf{c}g'(\zeta_t)]\frac{s}{l_j}ds\} \quad (104)$$

Thus, the surface traction-charge and EDEP induced by the temperature discontinuity are of the form

$$\mathbf{t}_n^0(s) = \Pi_i n_i = \sum_{j=1}^{M}(\mathbf{x}_j n_1 + \mathbf{y}_j n_2)\hat{T}_j,\quad \mathbf{u}_*^0(s) = \sum_{j=1}^{M}\mathbf{w}_j(s)\hat{T}_j \quad (105)$$

In general, $\mathbf{t}_n^0(s) \neq 0$ over Γ_t (the boundary on which SED is prescribed) and $\mathbf{u}_*^0(s) \neq 0$ over Γ_u (the boundary on which EDEP is prescribed). To satisfy the SED (or EDEP) on the corresponding boundaries, we must superpose a solution of the corresponding isothermal problem with a SED (or a EDEP) equal and opposite to those of Eq. (105). The details will be given in the following sub-section.

IV.2.2 BEM for EDEP discontinuity problem

Consider again the domain Ω_1, the governing equation and its boundary conditions are described as follows

$$\Pi_{ij,j} = 0 \quad \text{in } \Omega_1 \quad (106)$$

$$t_{ni} = \Pi_{ij}n_j = t_i^0 - (\mathbf{t}_n^0)_i \quad \text{on } \Gamma_t \quad (107)$$

$$u_i = u_i^0 - (\mathbf{u}_*^0)_i \quad \text{on } \Gamma_u \quad (108)$$

$$\begin{aligned} &t_{ni}\big|_{L^+} = -t_{ni}\big|_{L^-} = -(\mathbf{t}_n^0)_i, \\ &\hat{u}_i = u_i\big|_{L^+} - u_i\big|_{L^-} - (\mathbf{u}_*^0)_i\big|_{L^+} + (\mathbf{u}_*^0)_i\big|_{L^-} \end{aligned} \quad \text{on } L \quad (109)$$

where Γ_t and Γ_u are the boundaries on which the prescribed values of SED t_i^0 and EDEP u_i^0 are imposed, and $\Pi_{ij} = (\boldsymbol{\Pi}_j)_i$. Similarly, the total potential energy for the electroelastic problem can be given as

$$\Pi(\hat{\mathbf{u}}) = \frac{1}{2}\int_L[\boldsymbol{\phi}(\hat{\mathbf{u}})\cdot\hat{\mathbf{u}}_{,s} + 2\mathbf{t}_n^0\cdot\hat{\mathbf{u}}]ds - \int_\Gamma(\mathbf{t}^0 - \mathbf{t}_n^0)\cdot\hat{\mathbf{u}}ds \quad (110)$$

where the elastic solutions of the functions $\boldsymbol{\phi}(\hat{\mathbf{u}})$ and $\mathbf{u}(\hat{\mathbf{u}})$ have been given in [46]. These solutions are:

$$\begin{aligned}\mathbf{u}(\hat{\mathbf{u}}) &= \frac{1}{\pi}\mathrm{Im}[\mathbf{A}\langle\ln(\zeta_\alpha - \zeta_{\alpha 0})\rangle\mathbf{B}^T\hat{\mathbf{u}} \\ &+ \frac{1}{\pi}\sum_{\beta=1}^{4}\mathrm{Im}[\mathbf{A}\langle\ln(\zeta_\alpha^{-1} - \bar{\zeta}_{\beta 0})\rangle\mathbf{B}^{-1}\bar{\mathbf{B}}\mathbf{I}_\beta\bar{\mathbf{B}}^T\hat{\mathbf{u}}\end{aligned} \quad (111)$$

$$\begin{aligned}\boldsymbol{\phi}(\hat{\mathbf{u}}) &= \frac{1}{\pi}\mathrm{Im}[\mathbf{B}\langle\ln(\zeta_\alpha - \zeta_{\alpha 0})\rangle\mathbf{B}^T\hat{\mathbf{u}} \\ &+ \frac{1}{\pi}\sum_{\beta=1}^{4}\mathrm{Im}[\mathbf{B}\langle\ln(\zeta_\alpha^{-1} - \bar{\zeta}_{\beta 0})\rangle\mathbf{B}^{-1}\bar{\mathbf{B}}\mathbf{I}_\beta\bar{\mathbf{B}}^T\hat{\mathbf{u}}\end{aligned} \quad (112)$$

where

$$\begin{aligned}&\mathbf{I}_1 = \mathrm{diag}[1,0,0,0],\quad \mathbf{I}_2 = \mathrm{diag}[0,1,0,0], \\ &\mathbf{I}_3 = \mathrm{diag}[0,0,1,0],\quad \mathbf{I}_4 = \mathrm{diag}[0,0,0,1]\end{aligned} \quad (113)$$

As before the boundaries L and Γ are divided into a series of boundary elements, for which the EDEP discontinuity may be approximated through linear interpolation as

$$\hat{\mathbf{u}}(s) = \hat{\mathbf{u}}_m F_m(s) + \hat{\mathbf{u}}_{m+1}F_{m+1}(s) \quad (114)$$

With approximation (114), the EDEP and SED functions given in Eqs. (111) and (112) can now be expressed by

$$\mathbf{u}(\boldsymbol{\zeta}) = \sum_{m=1}^{M}\mathrm{Im}[\mathbf{A}\mathbf{D}_m(\boldsymbol{\zeta})]\hat{\mathbf{u}}_m,\quad \boldsymbol{\phi}(\boldsymbol{\zeta}) = \sum_{m=1}^{M}\mathrm{Im}[\mathbf{B}\mathbf{D}_m(\boldsymbol{\zeta})]\hat{\mathbf{u}}_m \quad (115)$$

where

$$\mathbf{D}_m(\boldsymbol{\zeta}) = \frac{1}{\pi}\int_{l_{m-1}}\{\langle\ln(\zeta_\alpha - \zeta_{\alpha 0}^{m-1})\rangle\mathbf{B}^T + \sum_{\beta=1}^{4}\langle\ln(\zeta_\alpha^{-1} - \bar{\zeta}_{\beta 0}^{m-1})\rangle\mathbf{B}^{-1}\bar{\mathbf{B}}\mathbf{I}_\beta\bar{\mathbf{B}}^T\}\frac{l_{m-1}-s}{l_{m-1}}ds$$
$$+\frac{1}{\pi}\int_{l_m}\{\langle\ln(\zeta_\alpha - \zeta_{\alpha 0}^{m})\rangle\mathbf{B}^T + \sum_{\beta=1}^{4}\langle\ln(\zeta_\alpha^{-1} - \bar{\zeta}_{\beta 0}^{m})\rangle\mathbf{B}^{-1}\bar{\mathbf{B}}\mathbf{I}_\beta\bar{\mathbf{B}}^T\}\frac{s}{l_m}ds \quad (116)$$

in which ζ_t and ζ_{t0} can be expressed in terms of s by the relations

$$z_\alpha = f(\zeta_\alpha) = a(a_{1\alpha}\zeta_\alpha + a_{2\alpha}\zeta_\alpha^{-1} + e_{n1}a_{3\alpha}\zeta_\alpha^{n} + e_{n1}a_{4\alpha}\zeta_\alpha^{-n}) \quad (117)$$

$$\zeta_{\alpha 0}^{\text{m-1}} = f^{-1}(z_{\alpha 0}^{m-1}), \qquad \zeta_{\alpha 0}^{m} = f^{-1}(z_{\alpha 0}^{m}), \quad (118)$$

$$z_{\alpha 0}^{m-1} = d_{\alpha m} + s(\cos\alpha_{m-1} + p_\alpha \sin\alpha_{m-1}),$$
$$z_{\alpha 0}^{m} = d_{\alpha m} + s(\cos\alpha_{m} + p_\alpha \sin\alpha_{m}) \quad (119)$$

and $d_{\alpha m} = x_{1m} + p_\alpha x_{2m}$.

In particular the displacement at node *j* is given by

$$\mathbf{u}(\zeta_0^j) = \sum_{m=1}^{M} \text{Im}[\mathbf{A}\mathbf{D}_m(\zeta_0^j)]\hat{\mathbf{u}}_m, \quad (120)$$

Substituting Eq. (44) into Eq. (39), we have

$$\Pi(\hat{\mathbf{u}}) = \sum_{i=1}^{M}[\hat{\mathbf{u}}_i^T \cdot (\sum_{j=1}^{M}\mathbf{k}_{ij}\hat{\mathbf{u}}_j)/2 - \mathbf{g}_i] \quad (121)$$

where

$$\mathbf{k}_{ij} = \frac{1}{l_{j-1}}\int_{l_{j-1}} \text{Im}[\mathbf{D}_i^T(\zeta_0^{j-1})\mathbf{B}^T]ds - \frac{1}{l_j}\int_{l_j} \text{Im}[\mathbf{D}_i^T(\zeta_0^{j})\mathbf{B}^T]ds \quad (122)$$

$$\mathbf{g}_j = \int_{l_{j-1}+l_j} \mathbf{G}_j F_j(s)ds \quad (123)$$

and $\mathbf{G}_j = -\mathbf{t}_n^0$ when node j is located at the boundary *L*, $\mathbf{G}_j = \mathbf{t}^0 - \mathbf{t}_n^0$ for other nodes. The minimization of Eq. (121) leads to a set of linear equations

$$\sum_{j=1}^{M}\mathbf{K}_{ij}\hat{\mathbf{u}}_j = \mathbf{g}_i \quad (124)$$

Similarly, the final form of the linear equations to be solved is obtained by selecting the appropriate ones, from among Eqs. (120) and (124). Eq. (120) will be chosen for those nodes at which the EDEP is prescribed, and Eq. (124) for the other nodes. Once the EDEP discontinuity $\hat{\mathbf{u}}$ has been found, the SED at any point can be expressed by:

$$\Pi_1 = -\sum_{m=1}^{M}\text{Im}[\mathbf{B}\mathbf{P}\mathbf{D}'_m(\mathbf{z})]\hat{\mathbf{u}}_m, \ \Pi_2 = \sum_{m=1}^{M}\text{Im}[\mathbf{B}\mathbf{D}'_m(\mathbf{z})]\hat{\mathbf{u}}_m \quad (125)$$

Therefore the SED, $\mathbf{\Pi}_n$, in a coordinate system local to the crack line, is given by

$$\mathbf{\Pi}_n = \mathbf{\Phi}(\alpha)\{-\mathbf{\Pi}_1\sin\alpha + \mathbf{\Pi}_2\cos\alpha\}^T \quad (126)$$

where $\mathbf{\Phi}(\alpha)$ is defined by[4]

$$\mathbf{\Phi}(\alpha) = \begin{bmatrix} \cos\alpha & \sin\alpha & 0 & 0 \\ -\sin\alpha & \cos\alpha & 0 & 0 \\ 0 & 0 & 1 & 0 \\ 0 & 0 & 0 & 1 \end{bmatrix} \quad (127)$$

Using Eq. (126) we can evaluate the SED intensity factors by the following definition

$$\mathbf{K}(c) = \{K_{II}\ K_I\ K_{III}\ K_D\}^T = \lim_{r\to 0}\sqrt{2\pi r}\mathbf{\Pi}_n(r) \quad (128)$$

We can evaluate the SED intensity factors in several ways: by extrapolation, traction and J-integral formulae [15]. In our analysis, the first method is used to calculate the SED intensity factors in BEM. Here, $\mathbf{\Pi}_n$ at any two points (say A and B) ahead of a crack-tip is first derived and then substituting them into Eq. (128), we obtain

$$\mathbf{K}^A = \mathbf{\sigma}_n^A\sqrt{2\pi r_A}, \ \mathbf{K}^B = \mathbf{\sigma}_n^B\sqrt{2\pi r_B} \quad (129)$$

where r_A (or r_B) are the distance from crack-tip to point A (or B). Finally, the SED intensity factors **K** can be obtained by the linear extrapolation of $\mathbf{K}^A$ and $\mathbf{K}^B$ to the crack tip, that is

$$\mathbf{K} = \mathbf{K}^A - \frac{\mathbf{K}^B - \mathbf{K}^A}{r_B - r_A}r_A \quad (130)$$

V. Trefftz finite element for piezoelectric materials

V.1 Basic equations for TFEM of piezoelectricity

V.1.1 Basic field equations and boundary conditions

Consider a linear piezoelectric material, in which the differential governing equations in the Cartesian coordinates x_i (i=1,2,3) are given by

$$\sigma_{ij,j} + \bar{b}_i = 0, \quad D_{i,i} + \bar{q}_b = 0 \quad \text{in } \Omega \quad (131)$$

where σ_{ij} is the stress tensor, D_i is the electric displacement vector, a comma denotes partial differentiation with respect to the coordinate x_i, $\bar{b}_i$ is the body force vector, $\bar{q}_b$ is the electric charge density, Ω is the solution domain, and the Einstein summation convention over repeated indices is used. For an anisotropic piezoelectric material, the constitutive relation is

$$\varepsilon_{ij} = -\frac{\partial H(\mathbf{\sigma},\mathbf{D})}{\partial \sigma_{ij}} = s_{ijkl}^D\sigma_{kl} + g_{kij}D_k$$
$$E_i = \frac{\partial H(\mathbf{\sigma},\mathbf{D})}{\partial D_i} = -g_{ikl}\sigma_{kl} + \lambda_{ik}^\sigma D_k \quad (132)$$

for $(\mathbf{\sigma},\mathbf{D})$ as basic variables,

$$\sigma_{ij} = \frac{\partial H(\mathbf{\varepsilon},\mathbf{E})}{\partial \varepsilon_{ij}} = c_{ijkl}^E\varepsilon_{kl} - e_{kij}E_k$$
$$D_i = -\frac{\partial H(\mathbf{\varepsilon},\mathbf{E})}{\partial E_i} = e_{ikl}\varepsilon_{kl} + \kappa_{ik}^\varepsilon E_k \quad (133)$$

for $(\mathbf{\varepsilon},\mathbf{E})$ as basic variables,

$$\sigma_{ij} = \frac{\partial H(\boldsymbol{\varepsilon}, \mathbf{D})}{\partial \sigma_{ij}} = c^D_{ijkl}\varepsilon_{kl} + h_{kij}D_k$$

$$E_i = \frac{\partial H(\boldsymbol{\varepsilon}, \mathbf{D})}{\partial D_i} = h_{ikl}\varepsilon_{kl} + \lambda^{\varepsilon}_{ik}D_k \qquad (134)$$

for $(\boldsymbol{\varepsilon}, \mathbf{D})$ as basic variables, and

$$\varepsilon_{ij} = -\frac{\partial H(\boldsymbol{\sigma}, \mathbf{E})}{\partial \sigma_{ij}} = s^E_{ijkl}\sigma_{kl} + d_{kij}D_k$$

$$D_i = -\frac{\partial H(\boldsymbol{\sigma}, \mathbf{E})}{\partial E_i} = d_{ikl}\sigma_{kl} + \kappa^{\sigma}_{ik}E_k \qquad (135)$$

for $(\boldsymbol{\sigma}, \mathbf{E})$ as basic variables, with

$$H(\boldsymbol{\sigma}, \mathbf{D}) = -\frac{1}{2}s^D_{ijkl}\sigma_{ij}\sigma_{kl} + \frac{1}{2}\lambda^{\sigma}_{ij}D_iD_j - g_{kij}\sigma_{ij}D_k \quad (136)$$

$$H(\boldsymbol{\varepsilon}, \mathbf{E}) = \frac{1}{2}c^E_{ijkl}\varepsilon_{ij}\varepsilon_{kl} - \frac{1}{2}\kappa^{\varepsilon}_{ij}E_iE_j - e_{kij}\varepsilon_{ij}E_k \quad (137)$$

$$H(\boldsymbol{\varepsilon}, \mathbf{D}) = \frac{1}{2}c^D_{ijkl}\varepsilon_{ij}\varepsilon_{kl} + \frac{1}{2}\lambda^{\varepsilon}_{ij}D_iD_j + h_{kij}\varepsilon_{ij}D_k \quad (138)$$

$$H(\boldsymbol{\sigma}, E) = -\frac{1}{2}s^E_{ijkl}\sigma_{ij}\sigma_{kl} - \frac{1}{2}\kappa^{\sigma}_{ij}E_iE_j - d_{kij}\sigma_{ij}E_k \quad (139)$$

where c^E_{ijkl}, c^D_{ijkl} and s^E_{ijkl}, s^D_{ijkl} are the stiffness and compliance coefficient tensor for **E**=0 or **D**=0, $\kappa^{\sigma}_{ij}, \kappa^{\varepsilon}_{ij}$ and $\lambda^{\sigma}_{ij}, \lambda^{\varepsilon}_{ij}$ are the permittivity matrix and the conversion of the permittivity constant matrix for $\boldsymbol{\sigma}$=0 or $\boldsymbol{\varepsilon}$=0, ε_{ij} and E_i are, respectively, the elastic strain tensor and the electric field intensity vector, e_{kij} is piezoelectric stress constants, g_{kij} is piezoelectric strain constants. These constants have the following relations:

$$\mathbf{c}^E = (\mathbf{s}^E)^{-1},\ \mathrm{e}=\mathbf{c}^{\mathrm{E}}\mathbf{d},\ \boldsymbol{\kappa}^{\varepsilon} = \boldsymbol{\kappa}^{\sigma} - \mathbf{d}^T\mathbf{c}^e\mathbf{d},$$
$$\mathbf{s}^D = (\mathbf{c}^E)^{-1} - \mathbf{d}(\boldsymbol{\kappa}^{\sigma})^{-1}\mathbf{d}^T,\ \mathbf{g} = \mathbf{d}(\boldsymbol{\kappa}^{\sigma})^{-1},$$
$$\mathbf{c}^D = \mathbf{c}^E - \mathbf{c}^E\mathbf{d}(\boldsymbol{\kappa}^{\varepsilon})^{-1}\mathbf{d}^T\mathbf{c}^E,\ \mathbf{h} = -\mathbf{c}^E\mathbf{d}(\boldsymbol{\kappa}^{\varepsilon})^{-1},$$
$$\boldsymbol{\lambda}^{\varepsilon} = (\boldsymbol{\kappa}^{\varepsilon})^{-1},\ \boldsymbol{\lambda}^{\sigma} = (\boldsymbol{\kappa}^{\sigma})^{-1} \qquad (140)$$

where superscript "*T*" denotes the transposition of a matrix.

The relation between the strain tensor and the displacement, u_i, is given by

$$\varepsilon_{ij} = \frac{1}{2}(u_{i,j} + u_{j,i}) \qquad (141)$$

and the electric field components are related to the electric potential ϕ by

$$E_i = -\phi_{,i} \qquad (142)$$

The boundary conditions of the boundary value problem (131)-(142) can be given by:

$$u_i = \bar{u}_i \qquad \text{on } \Gamma_u \qquad (143)$$

$$t_i = \sigma_{ij}n_j = \bar{t}_i \qquad \text{on } \Gamma_t \qquad (144)$$

$$D_n = D_in_i = -\bar{q}_n = \bar{D}_n \qquad \text{on } \Gamma_D \qquad (145)$$

$$\phi = \bar{\phi} \qquad \text{on } \Gamma_\phi \qquad (146)$$

where $\bar{u}_i, \bar{t}_i, \bar{q}_n$ and $\bar{\phi}$ are, respectively, prescribed boundary displacement, traction vector, surface charge and electric potential, an overhead bar denotes prescribed value, $\Gamma=\Gamma_u+\Gamma_t=\Gamma_D+\Gamma_\phi$ is the boundary of the solution domain Ω.

Moreover, in the Trefftz finite element form, eqns (131)-(146) should be completed by the following inter-element continuity requirements:

$$u_{ie} = u_{if},\quad \phi_e = \phi_f,\quad (\text{on } \Gamma_e \cap \Gamma_f, \text{ conformity}), \qquad (147)$$

$$t_{ie} + t_{if} = 0,\ D_{ne} + D_{nf} = 0\ (\text{on } \Gamma_e \cap \Gamma_f, \text{ reciprocity}) \qquad (148)$$

where '*e*' and '*f* ' stand for any two neighbouring elements. Equations (131)-(148) are taken as the basis to establish the modified variational principle for Trefftz finite element analysis of piezoelectric materials.

V.1.2

2.2 Assumed fields

The main idea of the TFEM is to establish a finite element (FE) formulation whereby the intra-element continuity is enforced on a non-conforming internal displacement field chosen so as to *a priori* satisfy the governing differential equation of the problem under consideration [95, 96]. In other words, as an obvious alternative to the Rayleigh-Ritz method as a basis for a FE formulation, the model here is based on the method of Trefftz. With this method the solution domain Ω is subdivided into elements, and over each element "*e*," the assumed intra-element fields are

$$\mathbf{u} = \begin{Bmatrix} u_1 \\ u_2 \\ u_3 \\ \phi \end{Bmatrix} = \begin{Bmatrix} \breve{u}_1 \\ \breve{u}_2 \\ \breve{u}_3 \\ \breve{\phi} \end{Bmatrix} + \begin{Bmatrix} \mathbf{N}_1 \\ \mathbf{N}_2 \\ \mathbf{N}_3 \\ \mathbf{N}_4 \end{Bmatrix}\mathbf{c} = \breve{\mathbf{u}} + \mathbf{N}\mathbf{c} \qquad (149)$$

where $\mathbf{c}_i$ stands for undetermined coefficient, and $\breve{\mathbf{u}}$ (= $\{\breve{u}_1, \breve{u}_2, \breve{u}_3, \breve{\phi}\}^T$) and **N** are known functions. If the governing differential equation (131) is rewritten in a general form

$$\Re\mathbf{u}(\mathbf{x}) + \bar{\mathbf{b}}(\mathbf{x}) = 0, \qquad (\mathbf{x} \in \Omega_e) \qquad (150)$$

where $\Re$ stands for the differential operator matrix for eqn (1), **x** for the position vector, $\bar{\mathbf{b}}$ (=$\{\{\bar{b}_1, \bar{b}_2, \bar{b}_3, \bar{q}_b\}^T$ for the known right-hand side term, the overhead bar

indicates the imposed quantities and Ω_e stands for the eth element sub-domain, then $\breve{\mathbf{u}} = \breve{\mathbf{u}}(\mathbf{x})$ and $\mathbf{N} = \mathbf{N}(\mathbf{x})$ in eqn (13) have to be chosen such that

$$\Re\breve{\mathbf{u}} + \bar{\mathbf{b}} = 0 \quad \text{and} \quad \Re\mathbf{N} = 0 \tag{151}$$

everywhere in Ω_e. The unknown coefficient **c** may be calculated from the conditions on the external boundary and/or the continuity conditions on the inter-element boundary. Thus various Trefftz element models can be obtained by using different approaches to enforce these conditions. In the majority of cases a hybrid technique is used, whereby the elements are linked through an auxiliary conforming displacement frame which has the same form as in the conventional FE method. This means that, in the Trefftz finite element approach, a conforming electric potential and displacement (EPD) field should be independently defined on the element boundary to enforce the field continuity between elements and also to link the coefficient **c**, appearing in Eq. (149), with nodal EPD **d** (=$\{d\}$). The frame is defined as

$$\tilde{\mathbf{u}}(\mathbf{x}) = \begin{Bmatrix} \tilde{u}_1 \\ \tilde{u}_2 \\ \tilde{u}_3 \\ \tilde{\phi} \end{Bmatrix} = \begin{Bmatrix} \tilde{\mathbf{N}}_1 \\ \tilde{\mathbf{N}}_2 \\ \tilde{\mathbf{N}}_3 \\ \tilde{\mathbf{N}}_4 \end{Bmatrix} \mathbf{d} = \tilde{\mathbf{N}}\mathbf{d}, \qquad (\mathbf{x} \in \Gamma_e) \tag{152}$$

where the symbol "~" is used to specify that the field is defined on the element boundary only, **d**=**d**(**c**) stands for the vector of the nodal displacements which are the final unknowns of the problem, Γ_e represents the boundary of element e, and $\tilde{\mathbf{N}}$ is a matrix of the corresponding shape functions which are the same as those in conventional FE formulation.

Using the above definitions the generalized boundary forces and electric displacements can be derived from Eqs. (141), (142) and (149), and denoted as

$$\mathbf{T} = \begin{Bmatrix} t_1 \\ t_2 \\ t_3 \\ D_n \end{Bmatrix} = \begin{Bmatrix} \sigma_{1j} n_j \\ \sigma_{2j} n_j \\ \sigma_{3j} n_j \\ D_j n_j \end{Bmatrix} = \begin{Bmatrix} \breve{t}_1 \\ \breve{t}_2 \\ \breve{t}_3 \\ \breve{D}_n \end{Bmatrix} + \begin{Bmatrix} \mathbf{Q}_1 \\ \mathbf{Q}_2 \\ \mathbf{Q}_3 \\ \mathbf{Q}_4 \end{Bmatrix} \mathbf{c} = \breve{\mathbf{T}} + \mathbf{Q}\mathbf{c} \tag{153}$$

where $\breve{t}_i$ and $\breve{D}_n$ are derived from $\breve{\mathbf{u}}$.

V.2 Modified variational principles

The Trefftz finite element equation for piezoelectric materials can be established by the variational approach [1]. Since the stationary conditions of the traditional potential and complementary variational functional cannot satisfy the inter-element continuity condition which is required in the Trefftz finite element analysis, some new variational functionals need to be developed. For this purpose, we present the following two modified variational functionals suitable for Trefftz finite element analysis:

$$\begin{aligned} \Pi_m^{\sigma D} = \sum_e \Pi_{me}^{\sigma D} = \sum_e \{ & \Pi_e^{\sigma D} - \int_{\Gamma_{De}} (\bar{D}_n - D_n)\tilde{\varphi} ds \\ & - \int_{\Gamma_{te}} (\bar{t}_i - t_i)\tilde{u}_i ds + \int_{\Gamma_{Ie}} (D_n \tilde{\varphi} + t_i \tilde{u}_i) ds \} \end{aligned} \tag{154}$$

$$\begin{aligned} \Pi_m^{\varepsilon E} = \sum_e \Pi_{me}^{\varepsilon E} = \sum_e \{ & \Pi_e^{\varepsilon E} + \int_{\Gamma_{\phi e}} (\bar{\phi} - \phi)\tilde{D}_n ds + \int_{\Gamma_{ue}} (\bar{u}_i - u_i)\tilde{t}_i ds \\ & - 2\int_{\Gamma_{te}} \tilde{u}_i t_i ds - 2\int_{\Gamma_{De}} \tilde{\phi} D_n ds - \int_{\Gamma_{Ie}} (\tilde{\phi} D_n + \tilde{u}_i t_i) ds \} \end{aligned} \tag{155}$$

$$\begin{aligned} \Pi_m^{\varepsilon D} = \sum_e \Pi_{me}^{\varepsilon D} = \sum_e \{ & \Pi_e^{\varepsilon D} - \int_{\Gamma_{De}} (\bar{D}_n - D_n)\tilde{\varphi} ds \\ & + \int_{\Gamma_{ue}} (\bar{u}_i - u_i)\tilde{t}_i ds - 2\int_{\Gamma_{te}} \tilde{u}_i t_i ds + \int_{\Gamma_{Ie}} (D_n \tilde{\varphi} - t_i \tilde{u}_i) ds \} \end{aligned} \tag{156}$$

$$\begin{aligned} \Pi_m^{\sigma E} = \sum_e \Pi_{me}^{\sigma E} = \sum_e \{ & \Pi_e^{\sigma E} + \int_{\Gamma_{\varphi e}} (\bar{\varphi} - \varphi)\tilde{D}_n ds \\ & - \int_{\Gamma_{te}} (\bar{t}_i - t_i)\tilde{u}_i ds - 2\int_{\Gamma_{De}} D_n \tilde{\varphi} ds - \int_{\Gamma_{Ie}} (D_n \tilde{\varphi} - t_i \tilde{u}_i) ds \} \end{aligned} \tag{157}$$

where

$$\Pi_e^{\sigma D} = \iint_{\Omega_e} H(\boldsymbol{\sigma}, \mathbf{D}) d\Omega + \int_{\Gamma_{ue}} t_i \bar{u}_i ds + \int_{\Gamma_{\varphi e}} D_n \bar{\varphi} ds \tag{158}$$

$$\begin{aligned} \Pi_e^{\varepsilon E} = & \iint_{\Omega_e} [H(\boldsymbol{\varepsilon}, \mathbf{E}) - \bar{b}_i u_i - \bar{q}_b \varphi] d\Omega \\ & + \int_{\Gamma_{te}} \bar{t}_i \tilde{u}_i ds + \int_{\Gamma_{De}} \bar{D}_n \tilde{\varphi} ds \end{aligned} \tag{159}$$

$$\begin{aligned} \Pi_e^{\varepsilon D} = & \iint_{\Omega_e} [H(\boldsymbol{\varepsilon}, \mathbf{D}) - \bar{b}_i u_i] d\Omega \\ & + \int_{\Gamma_{te}} \bar{t}_i \tilde{u}_i ds + \int_{\Gamma_{\varphi e}} D_n \bar{\varphi} ds \end{aligned} \tag{160}$$

$$\begin{aligned} \Pi_e^{\sigma E} = & \iint_{\Omega_e} [H(\boldsymbol{\sigma}, \mathbf{E}) - \bar{q}_b \varphi] d\Omega \\ & + \int_{\Gamma_{ue}} t_i \bar{u}_i ds + \int_{\Gamma_{De}} \bar{D}_n \tilde{\varphi} ds \end{aligned} \tag{161}$$

in which Eq. (131) is assumed to be satisfied, *a priori*. The terminology "modified principle" refers here to the use of a conventional functional (Π_e^{xy} here) and some modified terms for the construction of a special variational principle to account for additional requirements such as the condition defined in Eqs. (147) and (148).

The boundary Γ_e of a particular element consists of the following parts:

$$\Gamma_e = \Gamma_{ue} \cup \Gamma_{te} \cup \Gamma_{Ie} = \Gamma_{\phi e} \cup \Gamma_{De} \cup \Gamma_{Ie} \tag{162}$$

where

$$\Gamma_{ue}=\Gamma_u\cap\Gamma_e,\quad \Gamma_{te}=\Gamma_t\cap\Gamma_e,$$
$$\Gamma_{\varphi e}=\Gamma_\varphi\cap\Gamma_e,\quad \Gamma_{De}=\Gamma_D\cap\Gamma_e, \tag{163}$$

and Γ_{Ie} is the inter-element boundary of the element 'e'. We now show that the stationary condition of the functional (18) leads to Eqs. (143)-(148), $(u_i=\tilde{u}_i \text{ on } \Gamma_t)$ and $(\phi=\tilde{\phi} \text{ on } \Gamma_D)$, and present the theorem on the existence of extremum of the functional, which ensures that an approximate solution can converge to the exact one. Taking $\Pi_m^{\sigma D}$ as an example, we have the following two statements:

(a) *Modified complementary principle*

$$\delta\Pi_m^{\sigma D}=0 \Rightarrow (143)-(148) \tag{164}$$

where δ stands for the variation symbol.

(b) *Theorem on the existence of extremum*

If the expression

$$\iint_\Omega \delta^2 H(\boldsymbol{\sigma},\mathbf{D})d\Omega+\int_{\Gamma_t}\delta t_i\delta\tilde{u}_i ds+\int_{\Gamma_D}\delta D_n\delta\tilde{\phi}ds +\sum_e\int_{\Gamma_{Ie}}(\delta\tilde{\phi}\delta D_n+\delta\tilde{u}_i\delta t_i)ds \tag{165}$$

is uniformly positive (or negative) in the neighborhood of $\mathbf{u}_0$, where $\mathbf{u}_0$ is such a value that $\Pi_m^{\sigma D}(\mathbf{u}_0)=(\Pi_m^{\sigma D})_0$, and where $(\Pi_m^{\sigma D})_0$ stands for the stationary value of $\Pi_m^{\sigma D}$, we have

$$\Pi_m^{\sigma D}\geq(\Pi_m^{\sigma D})_0\ [\text{or}\ \Pi_m^{\sigma D}\leq(\Pi_m^{\sigma D})_0] \tag{166}$$

in which the relation that $\tilde{\mathbf{u}}_e=\tilde{\mathbf{u}}_f$ is identical on $\Gamma_e\cap\Gamma_f$ has been used.

PROOF: First, we derive the stationary conditions of functional (154). To this end, performing a variation of $\Pi_m^{\sigma D}$ and noting that Eq. (131) holds true *a priori* by the previous assumption, we obtain

$$\begin{aligned}\delta\Pi_m^{\sigma D}=&\int_{\Gamma_u}(\bar{u}_i-u_i)\delta t_i ds+\int_{\Gamma_\varphi}(\bar{\varphi}-\varphi)\delta D_n ds\\ &-\int_{\Gamma_t}[(\bar{t}_i-t_i)\delta\tilde{u}_i-(\tilde{u}_i-u_i)\delta t_i]ds\\ &-\int_{\Gamma_D}[(\bar{D}_n-D_n)\delta\tilde{\varphi}-(\tilde{\varphi}-\varphi)\delta D_n]ds\\ &+\sum_e\int_{\Gamma_{Ie}}[(\tilde{u}_i-u_i)\delta t_i+(\tilde{\varphi}-\varphi)\delta D_n+t_i\delta\tilde{u}_i+D_n\delta\tilde{\varphi}]ds\end{aligned} \tag{167}$$

Therefore, the Euler equations for expression (167) are Eqs. (143)-(148), $(u_i=\tilde{u}_i \text{ on } \Gamma_t)$ and $(\phi=\tilde{\phi} \text{ on } \Gamma_D)$, as the quantities δt_i, δu_i, $\delta\phi$, δD_n, $\delta\tilde{u}_i$ and $\delta\tilde{\phi}$ may be arbitrary. The principle (148) has thus been proved. This indicates that the stationary condition of the functional satisfies the required boundary and inter-element continuity equations and can thus be used for deriving Trefftz finite element formulation.

As for the proof of the theorem on the existence of extremum, we may complete it by way of the so-called "second variational approach". In doing this, performing variation of $\delta\Pi_m^{\sigma D}$ and using the constrained conditions (1), we find

$$\delta^2\Pi_m^{\sigma D}=\iint_\Omega\delta^2 H(\boldsymbol{\sigma},\mathbf{D})d\Omega+\int_{\Gamma_t}\delta t_i\delta\tilde{u}_i ds+\int_{\Gamma_D}\delta D_n\delta\tilde{\varphi}ds +\sum_e\int_{\Gamma_{Ie}}(\delta\tilde{\varphi}\delta D_n+\delta\tilde{u}_i\delta t_i)ds=\text{expression (165)} \tag{168}$$

Therefore the theorem has been proved from the sufficient condition of the existence of a local extreme of a functional [95]. This completes the proof.

V.3 Element stiffness matrix

The element matrix equation can be generated by setting $\delta\Pi_{me}^{xy}=0$. To simplify the derivation, we first transform all domain integrals in Eq. (154) into boundary ones. In fact, by reason of the solution properties of the intra-element trial functions, the functional $\Pi_{me}^{\sigma D}$ can be simplified to

$$\begin{aligned}\Pi_{me}^{\sigma D}=&-\frac{1}{2}\int_{\Gamma_e}(t_i u_i+D_n\phi)ds-\frac{1}{2}\int_\Omega(\bar{b}_i u_i+\bar{q}_b\phi)d\Omega-\int_{\Gamma_{De}}(\bar{D}_n-D_n)\tilde{\phi}ds\\ &-\int_{\Gamma_{te}}(\bar{t}_i-t_i)\tilde{u}_i ds+\int_{\Gamma_{Ie}}(D_n\tilde{\phi}+t_i\tilde{u}_i)ds+\int_{\Gamma_{ue}}t_i\bar{u}_i ds+\int_{\Gamma_{\phi e}}D_n\bar{\phi}ds\end{aligned} \tag{169}$$

Substituting the expressions given in Eqs. (149), (152), and (153) into (169) produces

$$\Pi_{me}^{\sigma D}=-\frac{1}{2}\mathbf{c}^T\mathbf{H}\mathbf{c}+\mathbf{c}^T\mathbf{S}\mathbf{d}+\mathbf{c}^T\mathbf{r}_1+\mathbf{d}^T\mathbf{r}_2+\text{terms without }\mathbf{c}\text{ or }\mathbf{d} \tag{170}$$

in which the matrices **H**, **S** and the vectors $\mathbf{r}_1$, $\mathbf{r}_2$ are defined by

$$\mathbf{H}=\int_{\Gamma_e}\mathbf{Q}^T\mathbf{N}ds$$

$$\mathbf{S}=\int_{\Gamma_{De}}\mathbf{Q}_4^T\tilde{\mathbf{N}}_4 ds+\int_{\Gamma_{te}}\begin{bmatrix}\mathbf{Q}_1\\ \mathbf{Q}_2\\ \mathbf{Q}_3\end{bmatrix}^T\begin{bmatrix}\tilde{\mathbf{N}}_1\\ \tilde{\mathbf{N}}_2\\ \tilde{\mathbf{N}}_3\end{bmatrix}ds+\int_{\Gamma_e}\mathbf{Q}^T\tilde{\mathbf{N}}ds$$

$$\mathbf{r}_1=-\frac{1}{2}\int_{\Gamma_e}(\mathbf{N}^T\bar{\mathbf{T}}+\mathbf{Q}^T\breve{\mathbf{u}})ds-\frac{1}{2}\int_\Omega\mathbf{N}^T\bar{\mathbf{b}}d\Omega +\int_{\Gamma_{\varphi e}}\mathbf{Q}_4^T\bar{\varphi}ds+\int_{\Gamma_{ue}}\begin{bmatrix}\mathbf{Q}_1\\ \mathbf{Q}_2\\ \mathbf{Q}_3\end{bmatrix}^T\begin{Bmatrix}\bar{u}_1\\ \bar{u}_2\\ \bar{u}_3\end{Bmatrix}ds$$

$$\mathbf{r}_2 = \int_{\Gamma_{De}} \tilde{\mathbf{N}}_4^T (\breve{D}_n - \bar{D}_n) ds + \int_{\Gamma_e} \tilde{\mathbf{N}}^T \breve{\mathbf{T}} ds + \int_{\Gamma_{te}} \begin{bmatrix} \tilde{\mathbf{N}}_1 \\ \tilde{\mathbf{N}}_2 \\ \tilde{\mathbf{N}}_3 \end{bmatrix}^T \left(\begin{Bmatrix} \breve{t}_1 \\ \breve{t}_2 \\ \breve{t}_3 \end{Bmatrix} - \begin{Bmatrix} \bar{t}_1 \\ \bar{t}_2 \\ \bar{t}_3 \end{Bmatrix} \right) ds$$

To enforce inter-element continuity on the common element boundary, the unknown vector **c** should be expressed in terms of nodal DOF **d**. An optional relationship between **c** and **d** in the sense of variation can be obtained from

$$\frac{\partial \Pi_{me}^{\sigma D}}{\partial \mathbf{c}^T} = -\mathbf{H}\mathbf{c} + \mathbf{S}\mathbf{d} + \mathbf{r}_1 = 0 . \tag{171}$$

This leads to

$$\mathbf{c} = \mathbf{G}\mathbf{d} + \mathbf{g} , \tag{172}$$

where $\mathbf{G} = \mathbf{H}^{-1}\mathbf{S}$ and $\mathbf{g} = \mathbf{H}^{-1}\mathbf{r}_1$, and then straightforwardly yields the expression of $\Pi_{me}^{\sigma D}$ only in terms of **d** and other known matrices

$$\Pi_{me}^{\sigma D} = \frac{1}{2}\mathbf{d}^T\mathbf{G}^T\mathbf{H}\mathbf{G}\mathbf{d} + \mathbf{d}^T(\mathbf{G}^T\mathbf{H}\mathbf{g} + \mathbf{r}_2) + \text{terms without } \mathbf{d} \tag{173}$$

Therefore, the element stiffness matrix equation can be obtained by taking the vanishing variation of the functional $\Pi_{me}^{\sigma D}$ as

$$\frac{\partial \Pi_{me}^{\sigma D}}{\partial \mathbf{d}^T} = 0 \Rightarrow \quad \mathbf{K}\mathbf{d} = \mathbf{P} \tag{174}$$

where $\mathbf{K}=\mathbf{G}^T\mathbf{H}\mathbf{G}$ and $\mathbf{P}=-\mathbf{G}^T\mathbf{H}\mathbf{g}-\mathbf{r}_2$ are, respectively, the element stiffness matrix and the equivalent nodal flow vector. The expression (174) is the elemental stiffness-matrix equation for Trefftz finite element analysis.

V.Conclusions and future developments

On the basis of the preceding discussion, following conclusions can be drawn. This review presents an overall view on modeling and analysis of piezoelectric materials. It spreads Green's function approach, fracture mechanics, functionally graded materials, boundary element, and finite element modeling.

It is recognized that study on piezoelectric materials becomes a hot topic and has become increasingly popular due their widely applications in engineering fields. However, there are still many possible extensions and areas in need of further development in the future. Among those developments one could list the following:

1 Development of efficient Trefftz finite element-boundary element method schemes for complex piezoelectric structures and the related general purpose computer codes with preprocessing and postprocessing capabilities.

2 Applications of piezoelectric materials to MEMS and smart devices and development of the associated design and fabrication approaches.

3 Extension of the Trefftz-finite element method to elastodynamics of piezoelectric structures, dynamics of thin and thick plate bending and fracture mechanics for structures containing piezoelectric sensor and actuators.

4 Development of multiscale framework across from continuum to micro- and nano-scales for modeling piezoelectric materials and structures.

References

[1] Curie J, Curie P. Development par compression de l'eletricite polaire dans les cristaux hemiedres a faces inclines. Comptes Rendus Acad Sci Paris 1880;91: 294.

[2] Voigt W. General theory of the piezo-and pyroelectric properties of crystals. Abh Gott 1890;36(1).

[3] Cady W. Piezoelectricity, vols. 1 and 2. New York: Dover Publishers; 1964.

[4] Tiersten HF. Linear piezoelectric plate vibrations. New York: Springer; 1969.

[5] Parton VZ, Kudryavtsev BA. Electromagnetoelasticity: piezoelectrics and electrically conductive solids. New York: Gordon and Breach Science Publishers; 1988.

[6] Ikeda T. Fundamentals of piezoelectricity. New York: Oxford university press; 1996.

[7] Rogacheva NN. The theory of piezoelectric shells and plates. Boca Raton: CRC Press; 1994.

[8] Qin QH. Fracture mechanics of piezoelectric materials: WIT Press, Southampton; 2001.

[9] Qin QH. Green's function and boundary elements of multifield materials: Elsevier, Oxford; 2007.

[10] Qin QH. Advanced mechanics of piezoelectricity: Higher Education Press and Springer, Beijing; 2013.

[11] Qin QH. Mechanics of Cellular Bone Remodeling: Coupled Thermal, Electrical, and Mechanical Field Effects: CRC Press, Taylor & Francis, Boca Raton; 2013.

[12] Qin QH, Yang QS. Macro-micro theory on multifield coupling behaivor of hetereogenous materials: Higher Education Press and Springer, Beijing; 2008.

[13] Diao S, Qin QH, Dong J. On branched interface cracks between two piezoelectric materials. Mechanics research communications 1996;23(6): 615-20.

[14] Qin QH, Mai YW. Crack branch in piezoelectric bimaterial system. International Journal of Engineering Science 2000;38(6): 673-93.

[15] Qin QH, Zhang X. Crack deflection at an interface between dissimilar piezoelectric materials. International Journal of Fracture 2000;102(4): 355-70.

[16] Fu D, Hou Z, Qin QH, Xu L, Zeng Y. Influence of Shear Stress on Behaviors of Piezoelectric Voltages in Bone. Journal of Applied Biomechanics 2012;28(4): 387-93.

[17] Fu DH, Hou ZD, Qin QH. Analysis of the waveforms of piezoelectric voltage of bone. Journal of Tianjin University 2006;39: 349-53.

[18] Fu DH, Hou ZD, Qin QH. Influence of a notch on the piezoelectric voltages in bone. Engineering Mechanics 2011;28(1): 233-37.
[19] Fu DH, Hou ZD, Qin QH, Lu C. On the Influence of Relative Humidity on Piezoelectric Signals in Bone. Journal of Experimental Mechanics 2009;24(5): 473-78.
[20] Hou Z, Fu D, Qin QH. An exponential law for stretching–relaxation properties of bone piezovoltages. International Journal of Solids and Structures 2011;48(3): 603-10.
[21] Xu L, Hou Z, Fu D, Qin Q-H, Wang Y. Stretched exponential relaxation of piezovoltages in wet bovine bone. Journal of the Mechanical Behavior of Biomedical Materials 2015;41: 115-23.
[22] He X, Qu C, Qin QH. A theoretical model for surface bone remodeling under electromagnetic loads. Archive of Applied Mechanics 2008;78(3): 163-75.
[23] Qin QH. Thermoelectroelastic solutions for internal bone remodelling under constant loads. Mechanics of electromagnetic solids 2003;3: 73-88.
[24] Qin QH. Multi-field bone remodeling under axial and transverse loads. In: Boomington DR, editor. New research on biomaterials. New York: Nova Science Publishers; 2007. 49-91.
[25] Qin QH, Qu C, Ye J. Thermoelectroelastic solutions for surface bone remodeling under axial and transverse loads. Biomaterials 2005;26(33): 6798-810.
[26] Qin QH, Ye JQ. Thermoelectroelastic solutions for internal bone remodeling under axial and transverse loads. International Journal of Solids and Structures 2004;41(9): 2447-60.
[27] Qu C, He X, Qin QH. Bone functional remodeling under multi-field loadings. Proceedings of the 5th Australasian Congress on Applied Mechanics 2007: 627-32.
[28] Qu C, Qin QH. Bone remodeling under multi-field coupled loading. Zhineng Xitong Xuebao(CAAI Transactions on Intelligent Systems) 2007;2(3): 52-58.
[29] Qu C, Qin QH, Kang Y. A hypothetical mechanism of bone remodeling and modeling under electromagnetic loads. Biomaterials 2006;27(21): 4050-57.
[30] He X, Wang JS, Qin QH. Saint-Venant decay analysis of FGPM laminates and dissimilar piezoelectric laminates. Mechanics of Materials 2007;39(12): 1053-65.
[31] Hu KQ, Kang YL, Qin QH. A moving crack in a rectangular magnetoelectroelastic body. Engineering Fracture Mechanics 2007;74(5): 751-70.
[32] Hu KQ, Qin QH, Kang YL. Anti-plane shear crack in a magnetoelectroelastic layer sandwiched between dissimilar half spaces. Engineering Fracture Mechanics 2007;74(7): 1139-47.
[33] Qin QH. Solving anti-plane problems of piezoelectric materials by the Trefftz finite element approach. Computational Mechanics 2003;31(6): 461-68.
[34] Liu HY, Qin QH, Mai YW. Theoretical model of piezoelectric fibre pull-out. International Journal of Solids and Structures 2003;40(20): 5511-19.
[35] Qin QH, Wang JS, Kang YL. A theoretical model for electroelastic analysis in piezoelectric fibre push-out test. Archive of Applied Mechanics 2006;75(8-9): 527-40.
[36] Wang JS, Qin QH. Debonding criterion for the piezoelectric fibre push-out test. Philosophical Magazine Letters 2006;86(2): 123-36.
[37] Wang JS, Qin QH, Kang YL. Stress and electric field transfer of piezoelectric fibre push-out under electrical and mechanical loading. Proc of 9th International Conference on Inspection, Appraisal, Repairs & Maintenance of Structures, Fuzhou, China, 20-21 October: CI-Premier PTY LTD, ISBN: 981-05-3548-1; 2005. 435-42.
[38] Liu Z, Hou Z, Qin QH, Yu Y, Tang L. On electromechanical behaviour of frog sartorius muscles. Engineering in Medicine and Biology Society, 2005 IEEE-EMBS 2005 27th Annual International Conference of the: IEEE; 2006. 1252-55.
[39] Qin QH. Using GSC theory for effective thermal expansion and pyroelectric coefficients of cracked piezoelectric solids. International Journal of Fracture 1996;82(3): R41-R46.
[40] Qin QH, Mai YW, Yu SW. Effective moduli for thermopiezoelectric materials with microcracks. International Journal of Fracture 1998;91(4): 359-71.
[41] Qin QH, Yu SW. Effective moduli of piezoelectric material with microcavities. International Journal of Solids and Structures 1998;35(36): 5085-95.
[42] Qin QH, Yu SW. Using Mori-Tanaka method for effective moduli of cracked thermopiezoelectric materials. ICF 9-Sydney, Australia-19971997.
[43] Qin QH. Thermoelectroelastic Green's function for a piezoelectric plate containing an elliptic hole. Mechanics of Materials 1998;30(1): 21-29.
[44] Qin QH. Thermoelectroelastic Green's function for thermal load inside or on the boundary of an elliptic inclusion. Mechanics of Materials 1999;31(10): 611-26.
[45] Qin QH. Green's function for thermopiezoelectric plates with holes of various shapes. Archive of Applied Mechanics 1999;69(6): 406-18.
[46] Qin QH. Green function and its application for a piezoelectric plate with various openings. Archive of Applied Mechanics 1999;69(2): 133-44.
[47] Qin QH. Green's functions of magnetoelectroelastic solids with a half-plane boundary or bimaterial interface. Philosophical Magazine Letters 2004;84(12): 771-79.
[48] Qin QH. 2D Green's functions of defective magnetoelectroelastic solids under thermal loading. Engineering Analysis with Boundary Elements 2005;29(6): 577-85.
[49] Qin QH. Green's functions of magnetoelectroelastic solids and applications to fracture analysis. Proc of 9th International Conference on Inspection, Appraisal, Repairs & Maintenance of Structures, Fuzhou, China, 20-21 October,2005: CI-Premier PTY LTD, ISBN: 981-05-3548-1; 2005. 93-106.
[50] Qin QH, Mai YW. Thermoelectroelastic Green's function and its application for bimaterial of piezoelectric materials. Archive of Applied Mechanics 1998;68(6): 433-44.
[51] Qin QH. General solutions for thermopiezoelectrics with various holes under thermal loading. International Journal of Solids and Structures 2000;37(39): 5561-78.
[52] Qin QH, Mai YW. A new thermoelectroelastic solution for piezoelectric materials with various openings. Acta Mechanica 1999;138(1): 97-111.
[53] Qin QH, Mai YW, Yu SW. Some problems in plane thermopiezoelectric materials with holes. International Journal of Solids and Structures 1999;36(3): 427-39.
[54] Qin QH. A new solution for thermopiezoelectric solid with an insulated elliptic hole. Acta Mechanica Sinica 1998;14(2): 157-70.
[55] Qin QH. Thermoelectroelastic analysis of cracks in piezoelectric half-plane by BEM. Computational Mechanics 1999;23(4): 353-60.
[56] Qin QH. Material properties of piezoelectric composites by BEM and homogenization method. Composite structures 2004;66(1): 295-99.

[57] Qin QH. Micromechanics-BE solution for properties of piezoelectric materials with defects. Engineering Analysis with Boundary Elements 2004;28(7): 809-14.
[58] Qin QH. Micromechanics-BEM Analysis for Piezoelectric Composites. Tsinghua Science & Technology 2005;10(1): 30-34.
[59] Qin QH. Boundary Element Method. In: Yang JS, editor. Special Topics in the Theory of Piezoelectricity. Cambridge Massachusetts: Springer; 2009. 137-68.
[60] Qin QH. Analysis of Piezoelectric Solids through Boundary Element Method. J Appl Mech Eng 2012;2(1): e113.
[61] Qin QH, Mai YW. BEM for crack-hole problems in thermopiezoelectric materials. Engineering Fracture Mechanics 2002;69(5): 577-88.
[62] Qin QH. Mode III fracture analysis of piezoelectric materials by Trefftz BEM. Structural Engineering and Mechanics 2005;20(2): 225-40.
[63] Qin QH. Thermopiezoelectric interaction of macro-and micro-cracks in piezoelectric medium. Theoretical and Applied Fracture Mechanics 1999;32(2): 129-35.
[64] Qin QH. Variational formulations for TFEM of piezoelectricity. International Journal of Solids and Structures 2003;40(23): 6335-46.
[65] Qin QH. Fracture Analysis of Piezoelectric Materials by Boundary and Trefftz Finite Element Methods. WCCM VI in conjunction with APCOM'04, Sept 5-10, 2004, Beijing, China 2004.
[66] Qin QH. Trefftz Plane Element of Piezoelectric Plate with p-Extension Capabilities. IUTAM Symposium on Mechanics and Reliability of Actuating Materials 2006: 144-53.
[67] Cao C, Qin QH, Yu A. Hybrid fundamental-solution-based FEM for piezoelectric materials. Computational Mechanics 2012;50(4): 397-412.
[68] Cao C, Yu A, Qin QH. A new hybrid finite element approach for plane piezoelectricity with defects. Acta Mechanica 2013;224(1): 41-61.
[69] Wang H, Qin QH. Fracture analysis in plane piezoelectric media using hybrid finite element model. International Conference of fracture2013.
[70] Qin QH, Lu M. BEM for crack-inclusion problems of plane thermopiezoelectric solids. International Journal for Numerical Methods in Engineering 2000;48(7): 1071-88.
[71] Qin QH. Thermoelectroelastic solution for elliptic inclusions and application to crack–inclusion problems. Applied Mathematical Modelling 2000;25(1): 1-23.
[72] Qin QH, Mai YW. Crack growth prediction of an inclined crack in a half-plane thermopiezoelectric solid. Theoretical and Applied Fracture Mechanics 1997;26(3): 185-91.
[73] Liu HY, Qin QH, Mai YW. Crack growth in composites with piezoelectric fibers. Proc of the Third Int Conf for Mesomechanics, Xi'an, China, June 13-16: Tsinghua Univ. Press, Vol. 1; 2000. 357-66.
[74] Qin QH, Mai YW. Multiple cracks in thermoelectroelastic bimaterials. Theoretical and Applied Fracture Mechanics 1998;29(2): 141-50.
[75] Qin QH, Mai YW. Thermal analysis for cracks near interfaces between piezoelectric materials. Localized Damage 1998: Fifth International Conference on Damage and Fracture Mechanics 1998: 13-22.
[76] Qin QH, Yu SW. An arbitrarily-oriented plane crack terminating at the interface between dissimilar piezoelectric materials. International Journal of Solids and Structures 1997;34(5): 581-90.
[77] Qin QH, Yu SW. On the plane piezoelectric problem of a loaded crack terminating at a material interface. Acta Mechanica Solida Sinica 1996;9: 151-58.
[78] Qin QH, Mai YW. A closed crack tip model for interface cracks in thermopiezoelectric materials. International Journal of Solids and Structures 1999;36(16): 2463-79.
[79] Qin QH, Mai YW. Crack path selection in piezoelectric bimaterials. Composite structures 1999;47(1): 519-24.
[80] Qin QH, Wang JS, Li X. Effect of elastic coating on fracture behaviour of piezoelectric fibre with a penny-shaped crack. Composite structures 2006;75(1): 465-71.
[81] Wang JS, Qin QH. Penny-shaped Crack in a Solid Piezoelectric Cylinder With Two Typical Boundary Conditions. Journal of Beijing University of Technology 2006;32(S1): 29-34.
[82] Qin QH, Yu S. Logarithmic singularity at crack tips in piezoelectric media. Chinese science bulletin 1996;41(7): 563-66.
[83] Qiu W, Kang Y, Sun Q, Qin QH, Lin Y. Stress analysis and geometrical configuration selection for multilayer piezoelectric displacement actuator. Acta Mechanica Solida Sinica 2004;17(4): 323-29.
[84] Qiu W, Kang YL, Qin QH, Sun Q, Xu F. Study for multilayer piezoelectric composite structure as displacement actuator by Moire interferometry and infrared thermography experiments. Materials Science and Engineering: A 2007;452: 228-34.
[85] Wang JS, Qin QH. Symplectic model for piezoelectric wedges and its application in analysis of electroelastic singularities. Philosophical Magazine 2007;87(2): 225-51.
[86] Yang QS, Qin QH, Liu T. Interlayer stress in laminate beam of piezoelectric and elastic materials. Composite structures 2006;75(1): 587-92.
[87] Yang QS, Qin QH, Ma L, Lu X, Cui C. A theoretical model and finite element formulation for coupled thermo-electro-chemo-mechanical media. Mechanics of Materials 2010;42(2): 148-56.
[88] Yu SW, Qin QH. Damage analysis of thermopiezoelectric properties: Part I—crack tip singularities. Theoretical and Applied Fracture Mechanics 1996;25(3): 263-77.
[89] Yu SW, Qin QH. Damage analysis of thermopiezoelectric properties: Part II. Effective crack model. Theoretical and Applied Fracture Mechanics 1996;25(3): 279-88.
[90] Liu J, Liu X, Zhao Y. Green's functions for anisotropic magnetoelectroelastic solids with an elliptical cavity or a crack. International Journal of Engineering Science 2001;39(12): 1405-18.
[91] Gao C, Fan W. Green's functions for generalized 2D problems in piezoelectric media with an elliptic hole. Mechanics research communications 1998;25(6): 685-93.
[92] Pan E. Three-dimensional Green's functions in anisotropic magneto-electro-elastic bimaterials. Zeitschrift für angewandte Mathematik und Physik ZAMP 2002;53(5): 815-38.
[93] Yang JH, Lee KY. Penny-shaped crack in a piezoelectric cylinder under electro-mechanical loads. Archive of Applied Mechanics 2003;73(5-6): 323-36.
[94] Yang J, Lee K. Penny shaped crack in a three-dimensional piezoelectric strip under in-plane normal loadings. Acta Mechanica 2001;148(1-4): 187-97.
[95] Qin QH. The Trefftz finite and boundary element method. Southampton: WIT Press; 2000.
[96] Qin QH. Trefftz finite element method and its applications. Applied Mechanics Reviews 2005;58(5): 316-37.